2017-01-01

Experimental Investigation of Cryogenic Convection and Boiling in Traditionally and Additively Manufactured Rocket Engine Cooling Channels

Armando Sandoval
University of Texas at El Paso, asandovalramos1992@gmail.com

EXPERIMENTAL INVESTIGATION OF CRYOGENIC CONVECTION AND BOILING IN TRADITIONALLY AND ADDITIVELY MANUFACTURED ROCKET ENGINE COOLING CHANNELS

ARMANDO SANDOVAL JR

Master's Program in Mechanical Engineering

APPROVED:

Ahsan Choudhuri, Ph.D., Chair

Norman D. Love, Ph.D.

Luis Rene Contreras-Sapien, Ph.D.

Charles H. Ambler, Ph.D.
Dean of the Graduate School

Dedication

The following work is dedicated to my parents and brother, whose guidance, encouragement, and support have led me through the path of a successful academic career thus far.

EXPERIMENTAL INVESTIGATION OF CRYOGENIC CONVECTION AND BOILING IN TRADITIONALLY AND ADDITIVELY MANUFACTURED ROCKET ENGINE COOLING CHANNELS

By

ARMANDO SANDOVAL JR, B.S. Mechanical Engineering

THESIS

Presented to the Faculty of the Graduate School of

The University of Texas at El Paso

in Partial Fulfillment

of the Requirements

for the Degree of

MASTER OF SCIENCE

Department of Mechanical Engineering

THE UNIVERSITY OF TEXAS AT EL PASO

December 2017

Acknowledgements

I would like to express my sincere appreciation to my Graduate Advisor, Dr. Ahsan Choudhuri and Project Mentor, Charles Scott Hill, for their constant guidance and support that made this work possible. I am also grateful to the faculty and staff of the Mechanical Engineering Department at the University of Texas at El Paso, especially Dr. Norman Love, for providing me with astounding theoretical knowledge in the classroom that contributed to the successful completion of my graduate studies. Furthermore, this work would have not been possible without the financial support provided by NASA Johnson Space Center (JSC) under award No(s) NNX09AV09A. Special thanks goes to Dr. John C. Melcher from NASA JSC, whose mentorship and expertise played a key role in the completion of this work. I would also like to recognize my work colleagues at the Center for Space Exploration Technology Research; Enrique Gutierrez, Javier Chaparro, and Luz Bugarin, for their assistance and time invested in this project.

Abstract

The Center for Space Exploration and Technology Research at the University of Texas at El Paso, has designed, built, and optimized an experimental high heat flux test facility to investigate the heat transfer coefficient of liquid methane and other cryogenic propellants for regenerative cooled rocket engine design. The system is composed of a copper conduction based thermal concentrator that delivers heat flow into a single sub-scaled cooling channel (test article). This study focuses on optimizing this design of the high heat flux test facility to develop a more accurate method for measuring the conductive heat flow going into the cooling channel by adding an aluminum wafer between the copper block and test article, that will act as a thermal resistance of known geometry. Experimental repeatability for the upgraded set-up is validated based on previous experimental data collected for one copper test article with a 3.2 mm 3.2 mm squared cross-section geometry and a 0.8 μm surface roughness. It is important to note that this study uses LN_2 as its working fluid, and because the data used for comparison used LCH_4 as its working fluid, a non-dimensional number analysis was done prior to the present test in order to develop a test matrix that yields the necessary LN_2 flow rates and inlet properties. Moreover, this study will also provide a comparison of cooling effectiveness between traditionally manufactured and additively manufactured Inconel 625 squared cooling channels with different surface roughness. Data suggests that subcooled film-boiling phenomena is present in all channels tested, and film-boiling onset at critical heat flux (CHF) was correlated to the boiling number Bo ~ 0.056. Moreover, the convective Nusselt Number follows predicted trends for Reynolds Number with a wall temperature correction for both boiling and nonboiling regimes. Nusselt Number trends also suggest a higher heat transfer coefficient for channels with rougher surface finish. Nusselt number ranges are between 350 and 1450, while the Reynolds number ranges are between 195,000 and 245,000.

Table of Contents

List of Tables

List of Figures

Chapter 1: Introduction

1.1. Project Overview

Over the years, the idea of developing rocket fuel alternatives for deep space exploration has become a prominent area of research. In the field of bipropellant rocket engines, hydrocarbon fuels are receiving a significant amount of consideration for future vehicle propulsion systems due to their non-toxic chemical composition. More specifically, liquid methane has drawn a great deal of interest due to its weight efficiency, storage feasibility, and possibility for in-situ resource utilization [1]. These three advantages significantly improve a vehicle's mass and hence make the propellant useful for deep space missions with long duration periods. Due to the high temperatures reached during combustion however, the life of an engine is severely impacted by its cooling system's efficiency. Thus, in an effort to improve engine efficiency, regenerative cooling is presented as an alternative cooling method in which the energy absorbed by the cryogenic propellant is utilized to increase the initial energy of the propellant's content prior to injection. Figure 1.1 illustrates the only LOX/LCH_4 regenerative cooled engine that has been fired thus far.

Recent efforts from NASA's Johnson Space Center include the development of former Morpheus vehicle, which is an autonomous, planetary lander used to test liquid oxygen/liquid methane (LOX/Methane) propellant systems [2]. Furthermore, NASA is also aiming at developing a LOX/Methane regenerative cooled rocket engine to test with former Morpheus vehicle. In order to properly design a rocket engine regenerative cooled heat exchanger however, the heat transfer coefficient of the working propellant must be known. Although it is true that there exists plenty of data on the heat transfer characteristics of gaseous methane, there is a significant lack in such data for sub-critical liquid methane. Henceforth, the Center for Space Exploration and Technology Research at the University of Texas at El Paso has designed, built, and optimized an experimental

high heat flux test facility to investigate the heat transfer coefficient of liquid methane and other cryogenic propellants.

The high heat flux test facility serves as a high temperature environment simulator. It flows liquid cryogenic propellant through a single cooling channel that is heated by a copper conduction based thermal concentrator (block) on one side. This allows for the simulation of the one-dimensional, asymmetric heat flow experienced by the hot wall of a cooling channel in a regenerative cooled rocket engine and it further permits for the heat transfer characteristics of any liquid cryogenic propellant to be characterized and used for actual regenerative cooled rocket engine design. This simulation facility was developed between the years 2009 and 2011, and has since undergone design iterations over the past years in efforts of developing a more accurate method for quantifying the heat being transferred from the block onto the cooling channel. The following work presents a unique experimental design approach used to quantify the system's heat input into the cooling channel. Results are analyzed and compared to previous experimental data in order to strengthen experimental integrity and validate the system's heat transfer model.

Figure 1.1: XCOR XR-5M15 LOX/Methane Regenerative Cooled Engine [3]

1.2. Project Objectives

The purpose of this study is to ensure the proper functionality of an optimized high heat flux test facility by experimentally quantifying the heat transfer characteristics of subcritical liquid nitrogen (LN_2) using traditionally manufactured and additively manufactured sub-scaled single cooling channels at steady state conditions. In order to conduct this investigation, the scope of the experiment will be divided into two objectives.

The first objective will be to study the effects of surface roughness on cooling channels subjected to different temperatures. This will be done by generating Nusselt and Reynolds number correlations. During this study, one conventionally manufactured copper channel with a 0.8 μm surface roughness will be tested for validity of experimental repeatability. Additionally, three conventionally manufactured Inconel 625 channels with different surface roughness, and an additively manufactured Inconel 625 channel will be tested. The chosen surface finishes are later discussed and were chosen based on common surface finishes produced by milling [4]. It is expected that the cooling effectiveness will increase at the expense of increased pressure drops caused by the larger roughness finishes.

The second objective will be to conduct a boiling analysis to better observe the different modes of heat transfer (boiling and non-boiling). Furthermore, this analysis will better illustrate the point at which the critical heat flux (CHF) occurs along the length of the test section. The resulting data will be compared to previous studies and correlations generated. Similar trends will indicate a validation in experimental repeatability and confident proof conclusive in defining a more efficient heat transfer experimental model for the system. This would thus allow for further investigation on the heat transfer coefficient of different cryogenic propellants for use in actual regenerative cooled rocket engine design.

1.3. Experimental Approach

As already stated, all test article cooling channels will be heated using a conduction-based copper thermal concentrator (block). An aluminum wafer will be set atop of the copper block and the cooling channel's test section will be set atop of the aluminum wafer as shown in Figure 1.2. This stacking arrangement will allow for the three components to be in direct contact with each other and provide the cooling channel with a constant heat flux driven by the temperatures of the copper block. Furthermore, liquid nitrogen will be simultaneously flowing through the cooling channel while various temperature measurements are recorded. In order to validate the heat transfer phenomena, found in this experiment, both a conduction and convection analysis will be executed. The conduction analysis will be based on the aluminum wafer's geometric constraints and surface to surface temperature gradient, while the convection analysis will be focused on fluid flow characteristics and temperature gradient across the cooling channel. Ultimately, the results of these analyses will be evaluated to strengthen the integrity of the experimental set-up and allow for the comparison of data with previous experimental trials.

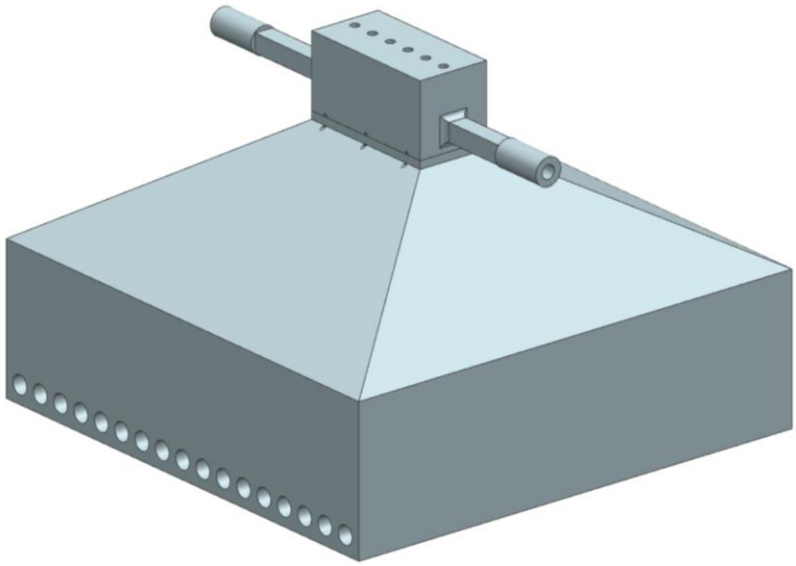

Figure 1.2: High Heat Flux Test Facility Stacking Arrangement

1.4. Relevance

In the past, the high heat flux test facility has been used to study the heat transfer characteristics of liquid methane. The conclusions attained from this study, may very well validate experimental repeatability and lead to future tests with different propellants. Furthermore, the methodology developed through this study, may also be applied to other channel geometries. This is extremely relevant for designers, to verify and/or build on different design requirements. Moreover, a properly functioning high heat flux test facility may also aid with validating several computational fluid dynamic models pertaining to the scope of this study. Overall, the relevance behind this experiment lies on its capability of quantifying the heat transfer coefficient of different cryogenic propellants and its flexibility in interchanging/testing different channel geometries for actual regen cooled rocket engine design.

Chapter 2: Literature Review

2.1 Hydrocarbon Fuels

Over the years, liquid oxygen/liquid hydrogen (LOX/LH2) has proven to be a very popular and successful bipropellant system in rocket engines. The problem with this propulsion system however, is that it requires a large amount of maintenance due to the inconvenient handling requirements that come with liquid hydrogen. This particular cryogenic propellant possesses a high density (0.0899 kg/m^3) and low cryogenic storage temperature (-253 °C) [1]. As a result, this propellant requires large storage tanks and a difficult protocol to maintain its liquid state. Moreover, the combustion products this system emits are toxic and harmful to the environment. For these reasons, recent studies have focused on investigating potential cost-effective propellants to be used in space applications. Hydrocarbon fuels are receiving a significant amount of consideration for future vehicle propulsion systems due to their non-toxic chemical composition. More specifically, liquid methane is of great interest due to its great storage capabilities and in-situ resource utilization possibilities.

Unlike liquid hydrogen, liquid methane possesses a low density (0.656 kg/m^3) and relatively high storage temperature (-161 °C), which is quite similar to that of its oxidizer, liquid oxygen (-183 °C) [1]. This in turn, allows for more propellant to be stored in smaller tanks without as much difficulty maintaining methane in its liquid form. Furthermore, the gases that are expelled by the reaction of methane and oxygen are considered non-toxic. An additional advantage to a LOX/Methane propulsion system is that it possesses in-situ resource utilization possibilities. This means that methane may actually be mined and created from space. As a result, extra tank storage on a space vehicle would no longer be required, making them more lightweight and ultimately more efficient for deep space exploration missions.

2.2 Regenerative Cooling

In liquid propellant engines, the use of cooling techniques is required to address the issue of high combustion temperatures. Because rocket fuel is usually stored as a cryogenic liquid, it may be used as a coolant for the engine. Regenerative cooling is the most preferred cooling method in high-thrust and high-pressure rocket engines because it increases its overall efficiency [5]. The regenerative heat exchanger uses multiple channels to flow the coolant (fuel) through the engine's contour from the nozzle exit of the thrust chamber to an exit near the injector face, as shown in Figure 2.1. This design thus allows for the energy absorbed to be utilized to augment the initial energy of the content of the propellant prior to injection. Hence, fuel-based regenerative cooling serves multiple purposes; it cools the engine and increases overall engine efficiency by absorbing energy along the way, prior to injection.

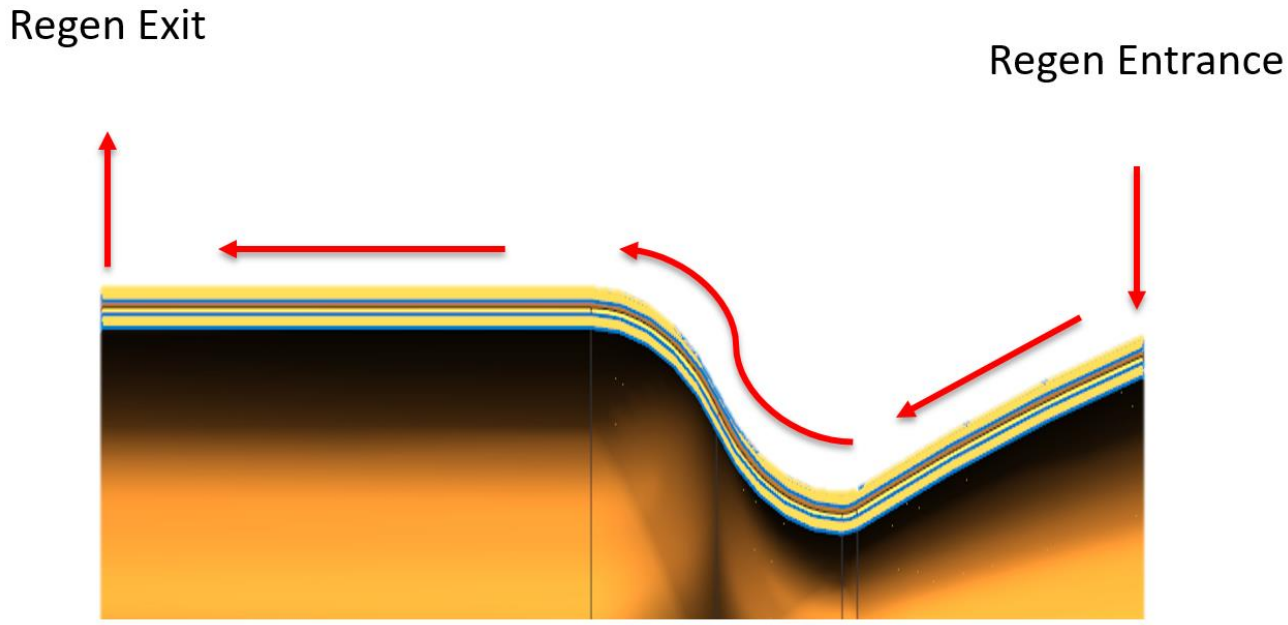

Figure 2.1: Cross Sectional View of Regenerative Cooling Passage

2.3 Additive Manufacturing for Regenerative Cooled Engines

One of the major drawbacks of a regenerative cooled engine design is its manufacturing complexity. Because the cooling channels are too small and abstract in geometry, traditional manufacturing methods are simply not adequate to yield the desired geometric parameters. Furthermore, the time required to manufacture such a product very much impacts manufacturing costs and project lead times. Whilst, additive manufacturing is presented as an alternative for manufacturing regenerative cooled rocket engine designs. This innovative manufacturing method "3-D prints" the engine and its cooling jacket contour in a matter of days, thus reducing manufacturing lead time and costs. Although this is in fact an efficient and cost-effective manufacturing method, the integrity of the material's mechanical properties is affected during the manufacturing process and must be assessed. In the case of a regenerative cooled rocket engine, experimental studies involving a high heat flux test facility are necessary in order to quantify the heat transfer coefficient to ensure that the additively manufactured test article exhibits high heat flux performance and high pressure drop.

2.4 Function of High Heat Flux Test Facilities

Different high heat flux test facilities have been developed over time to study the heat transfer characteristics of various liquid propellants and optimize the cooling capabilities of different regenerative cooled channel geometries. All designs flow the liquid propellant inside a single heated channel through internal forced convection. This procedure allows for an accurate simulation of the pressure and extreme temperature environments experienced by cooling channels in rocket engines. The main difference between high heat flux test facilities lies on their heating method. Some facilities use a resistive heating method, which produces circumferential heat flow throughout the channel. On the other hand, some facilities use a conductive heating method, which

involves one-sided, asymmetric flow through the cooling channel. In the case of simulating regenerative cooling channels, heat flow direction is crucial since the theoretical models used in design involve both a hot-wall side and cold-wall side temperature. Whilst, the ideal physical model to simulate would need to be a channel with both a hot-wall and cold-wall side, with one-dimensional, asymmetric heat flow experienced on the hot wall of a cooling channel.

2.5 Resistive Heated Facilities

Resistive heated facilities use a method known as ohmic heating. This heating method passes a current through a conductive metal, creating an exothermic release of energy in the form of heat. Although it is true that the heat flux going into the system may be easily controlled through this heating method, it also requires extremely high-power levels to reach the high heat fluxes experienced in a rocket engine. This may present a safety hazard, and point to extreme power requirements when dealing with certain materials. Furthermore, due to their heating method, resistive heated facilities will directly apply the current to the test article and evenly distribute the heat along the entire surface of the cooling channel [6]. Some examples of resistive heated facilities were investigated and are discussed below.

2.5.1 Heated Tube Facility by NASA John H. Glenn Research Center

In 2010, NASA Glenn Research Center conducted an investigation on the heat transfer characteristics of liquid and two-phase methane. The purpose of this test was to examine the response of the fuel when subjected to extreme conditions, similar to those experienced in the cooling channels of a rocket engine [5]. This task was accomplished by attaching copper bus bars to the test articles (cooling channels/tubes) to provide them with resistive power. Furthermore, the test article was placed inside of a vacuum chamber so as to reduce heat losses due to convection, and a total of fifteen thermocouples were spot welded on each test article, with the purpose of

providing a source for temperature monitoring during the test. Figure 2.2 illustrates the test article along with the thermocouple locations. AC reactors rated at 1500 amps provided the electrical power, and the maximum heat flux and temperature reached were 10.1 MW/m^2 and 726 °C respectively [6].

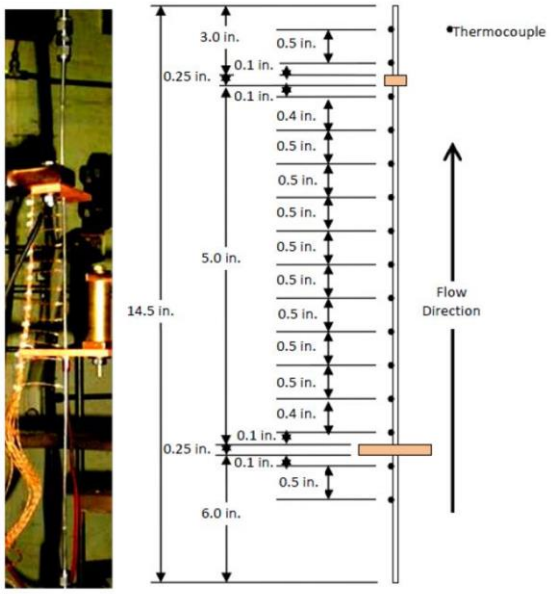

Figure 2.2: NASA Glenn Heated Tube Facility Experimental Set-Up and Schematic [6]

2.5.2 Electrically-Heated Tubular Test by Marshall Space Flight Center and Rocketdyne

During the mid-1980's, Rocketdyne embarked on a 12-month test campaign to study the heat transfer characteristics of liquid methane and liquid natural gas. The goal of this campaign, was to gain an understanding of the coking threshold and cooling capabilities of these fuels. In order to accomplish this task, copper samples were utilized so as to take advantage of the material's high thermal conductivity and allow the cooling channel to reach higher heat fluxes. The test article was placed inside of a high heat flux test facility developed at the Rockwell North American Aviation Operations (NAAO) Aerothermal Laboratory. This facility was originally designed to

accommodate single channel copper-based test articles under an environment similar to the one present in the chamber of the Space Shuttle Main Engine (SSME) [7]. The test articles were OHFC-copper surrounded by an Inconel K-500 reinforcement. AC reactors rated at 2000 amps provided the electrical power, and the maximum heat flux, wall temperature, and pressure were 139 MW/m^2, 482 °C, and 31 MPa respectively [7]. Figure 2.3 illustrates the experimental set-up.

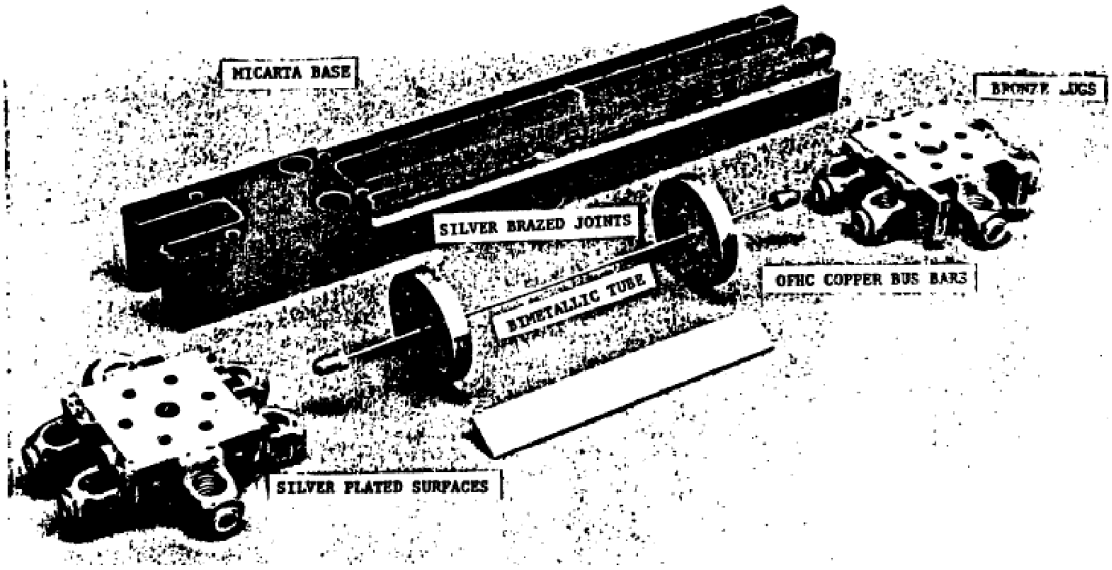

Figure 2.3: MSFC and Rocketdyne's High Heat Facility Experimental Set-Up [7]

2.6 Conductive Heated Facilities

Conduction-based heated facilities use a preheated thermal concentrator with a high thermal conductivity to conduct heat onto a test article. The interface between these two components is a constant contact area, which serves to deliver a constant heat flux into the test article. Unlike resistive heating, this method heats the cooling channel asymmetrically from one side and hence, better simulates the environment experienced in a rocket engine's regenerative cooling jacket by providing both a hot-wall and cold-wall side [8]. Furthermore, these facilities do not run the risk of potential tube material degradation that is also seen in resistively heated facilities

due to electrically driven chemical phenomena (high electrical currents). Some examples of studies done with conductive heated facilities were investigated and are presented below.

2.6.1 Aerojet Carbothermal Test Facility by Aerojet Technical Systems Corporation

During the late 1980's, Aerojet conducted a test campaign under the Hydrocarbon Fuel and Combustion Chamber Liner Materials Compatibility Program for NASA Lewis Research Center. The goal of this study, was to investigate the interactions between the fuel and combustion chamber, and develop a solution to avoid extreme corrosive damage on these materials. Test motivation came from a previous study done by the United Technologies Research Center and Rockwell International Rocketdyne Division, in which severe copper corrosion was observed when using restively heated tubes [8]. For this reason, Aerojet opted to use a conductive heated facility, which used a large copper block embedded with ten electrically insulated cartridge heaters as a thermal concentrator. The heat produced by the heaters is conducted through the copper block onto the test section, which consists of a small squared cooling channel milled at the bottom, as shown in Figure 2.4. Maximum heat flux, temperature, and pressure reached were 85 MW/m^2, 499 °C, and 24.1 MPa respectively [8].

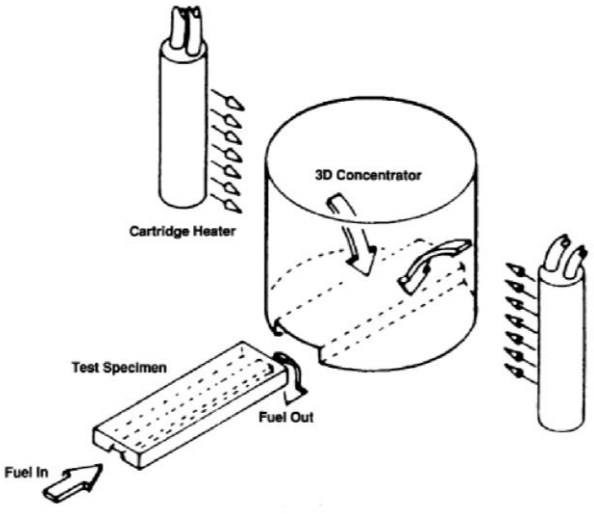

Figure 2.4: Aerojet Conductive Heated Facility Set-Up [8]

2.6.2 High Heat Flux Facility by Airforce Research Laboratory

In the years 2004 through 2007, the Airforce Research Laboratory led an investigation to study the heat transfer characteristics of hydrocarbon fuels experiencing the high temperatures found in regenerative cooling channels. This study was divided into two main goals; 1.) Designing a high heat flux facility that effectively delivers heat onto a test article, and 2.) Investigating the cross-sectional geometry effects of copper cooling channels on RP-2 fuel. In order to accomplish these tasks, the Airforce ran a series of Computational Fluid Dynamic simulations with different thermal concentrator geometries, as shown in Figure 2.5. The purpose of these simulations was to select a geometry configuration that best delivered heat onto the test sample and that allowed for the sample to be interchangeable [9].

Figure 2.5: Solid Geometries Simulated for Aerojet Study [9]

As seen on the figure above, all thermal concentrator geometries simulated include slots on top that accommodate cartridge heaters (inlet boundary condition). The outlet boundary condition used in the simulations was the convective heat transfer rate inside of the test article. Based on the simulation results, the Airforce opted to adapt a geometry configuration combining

their Solid 1 and Solid 3 geometries. The tapered section from Solid 1 would assist in geometrically focusing the heat input onto the test article, while the interchangeability from Solid 3 would allow for different channel geometries to be tested. In addition, the selected system was also place in a vacuum chamber so as to reduce convective heat losses and avoid oxidation of the copper. Figure 2.6 illustrates the assembly of the Airforce's High Heat Flux Facility. The maximum heat flux and pressure achieved by this system was 163.5 MW/m^2 and 31.0 MPa respectively [9].

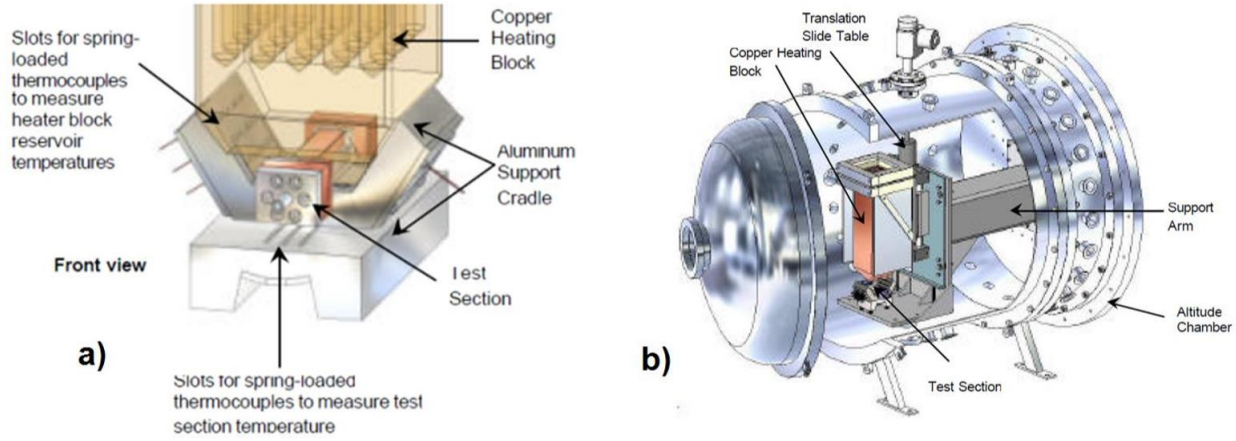

Figure 2.6: Components of Airforce High Heat Flux Facility [9]

2.6.3 High Heat Flux Test Facility by UTEP cSETR

The high heat flux test facility is a conduction based thermal concentrator system used to study the heat transfer characteristics of liquid methane for use in regenerative cooled rocket engine design. This system was developed by the Center for Space Exploration and Technology Research at the University of Texas at El Paso in the years ranging from 2009 to 2011, and it is an adaptation of the Airforce's High Heat Flux Facility discussed above [10]. It uses a copper block thermal concentrator that is heated using electrically resistive cartridge heaters inserted in the slots found at its bottom, and it accommodates a small rectangular test article on top, as shown in Figure

2.7. The contact interface between the copper block and the test article is a flat plane, which allows for even heat conduction distribution throughout the test article. Furthermore, a cradle is used alongside some nuts and threaded rods to act as a pressure mechanism pushing down on the assembly so as to reduce heat transfer losses due to conduction (poor contact between the block and test article). The complete system assembly is mounted on a test stand designed specifically for this copper block geometry configuration, and it is placed inside a vacuum chamber to reduce convection losses and oxidation of the copper. Maximum temperature and pressure achieved by this system is 275 °C and 2.05 MPa respectively [10].

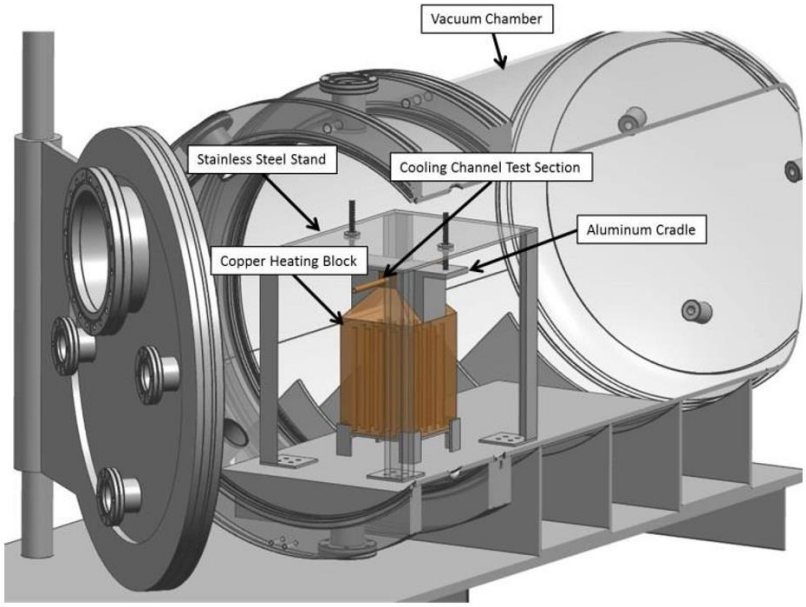

Figure 2.7: UTEP cSETR's High Heat Flux Test Facility [10]

Chapter 3: Development of Second Generation High Heat Flux Test Facility

3.1 Design Approach

The high heat flux test facility used in this study is an adaptation of the first-generation high heat flux test facility developed by the Center for Space Exploration and Technology Research at the University of Texas at El Paso discussed in the previous section. Although both facilities operate through a very similar procedure, a few modifications were made in an effort to avoid instrumentation failure and increase data accuracy. These modifications target the geometry of the copper block, heater placement, heater geometry/configuration, and the assembly of the facility as a whole. The following sections present the problems with the first-generation high heat flux test facility and the engineering justifications for the modifications made to this facility.

3.2 Problems with First-Generation High Heat Flux Test Facility

Although numerous successful tests were accomplished using the first-generation high heat flux test facility, some of its design attributes created test procedure inefficiencies, instrumentation failure, and potential data inaccuracies. These issues were identified and are discussed below, in an effort to show the need of an experimental design iteration (i.e. design of a second-generation high heat flux test facility).

3.2.1 Copper Block Geometry

In the first-generation high heat flux test facility, the copper thermal concentrator geometry was a 4” x 4” x 7” copper block with a 45-degree tapered section (trapezoidal pyramid) on top designed to geometrically focus the conducted heat onto a 2” x 1” flat section, as shown in Figure 3.1. Heat was provided to this block by electrical cartridge heaters that were inserted in 25 slots found on its bottom surface, however, because this placement subjected the heaters to gravity, epoxy cement was used to keep them in place. Furthermore, although the tapered section atop of

the copper block allowed for a more focused heat transfer, it also made it difficult to measure the actual heat flux going into the channel due the abstract trapezoidal pyramid geometry. This measurement process required the development of a heat transfer model involving Fourier's law of conduction to obtain the overall heat transfer rate through the entire high heat flux test facility and into the channel. In order to execute this model, assumptions were made that potentially affected experimental accuracy.

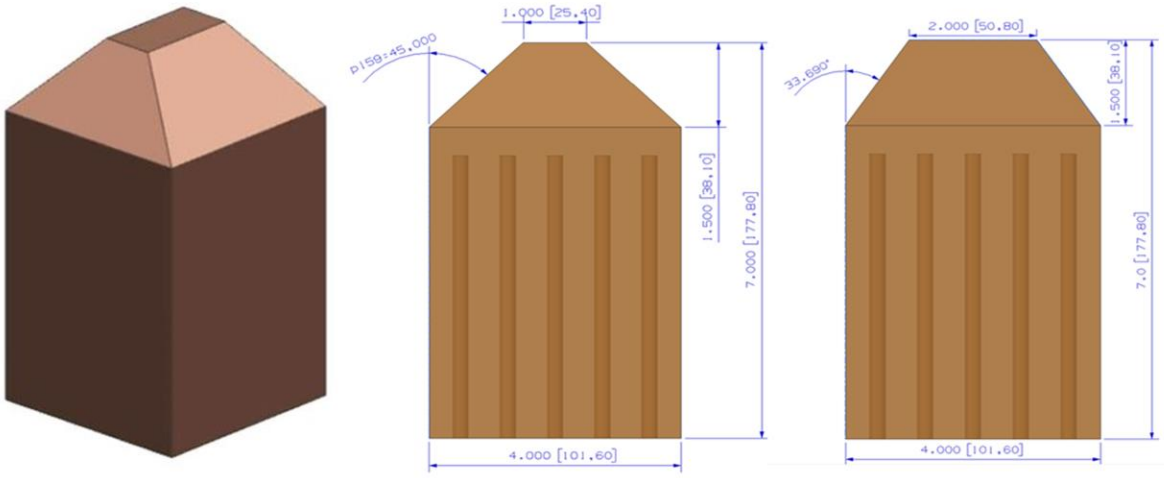

Figure 3.1: Copper Block Geometry for First Generation High Heat Flux Test Facility [11]

3.2.2 Electrical Cartridge Heaters

The sole purpose of the cartridge heaters in this high heat flux facility is to provide heat to the test article through conduction. In essence, the embedded cartridge heaters draw current from a power supply and convert it to heat that is then conducted through the copper block and into the test article. Resistive cartridge heaters, however, pose the great failure risk if not used properly. The most common cause of cartridge heater failure is an improper fit in the hole into which it is inserted. If the heater cannot dissipate the heat being generated and produced by contact with the sheath, the temperature inside the heater will continue to rise until the heater overheats and ultimately fails. Furthermore, each cartridge heater has a different watt rating that contributes to

the overall heat distribution in the system. In the case of this experimental set-up, this means that it is possible to over-equip the set-up with more than necessary cartridge heaters and produce more heat than the working cryogenic is capable of absorbing before vaporizing. In the first-generation high heat flux test facility, cartridge heater failure and cryogenic fluid vaporization were observed. As a result, a close analysis was executed on the sizing and selection of resistive cartridge heaters for the second-generation high heat flux test facility.

3.3 Design of Block for Second-Generation High Heat Flux Test Facility

The Second-Generation High Heat Flux Test Facility (HHFTF) consists of a shorter copper based thermal concentrator with 17 cartridge heater slots, an aluminum wafer, and a test sample, as shown in Figure 3.2. The block's geometry has been altered to allow the heaters to be inserted sideways rather than vertically thus eliminating the risk of slippage due to gravity during testing. Furthermore, the block's shorter geometry allows for the heat to concentrate and conduct more efficiently onto the test article atop. On another important note, because the thermal concentrator (block) used to deliver heat into the test sample still possesses a relatively abstract geometry, a method was designed to measure the heat flux going into the test sample. This method consists of a small piece of rectangular aluminum wafer that will be inserted between the block and the test sample as shown in the figure below. The aluminum's small thermal conductivity, relative to copper, will provide a large temperature difference (delta T) across the wafer, which will in turn make it simple to quantify the heat flux going into the test sample. The grooves found at the top of the copper block and at the bottom of the test sample are to accommodate the thermocouples that will provide the measurements necessary to compute the temperature difference across the aluminum wafer. Moreover, each test sample contains six thermocouple slots on top in order to monitor the temperature at different axial locations of the channel.

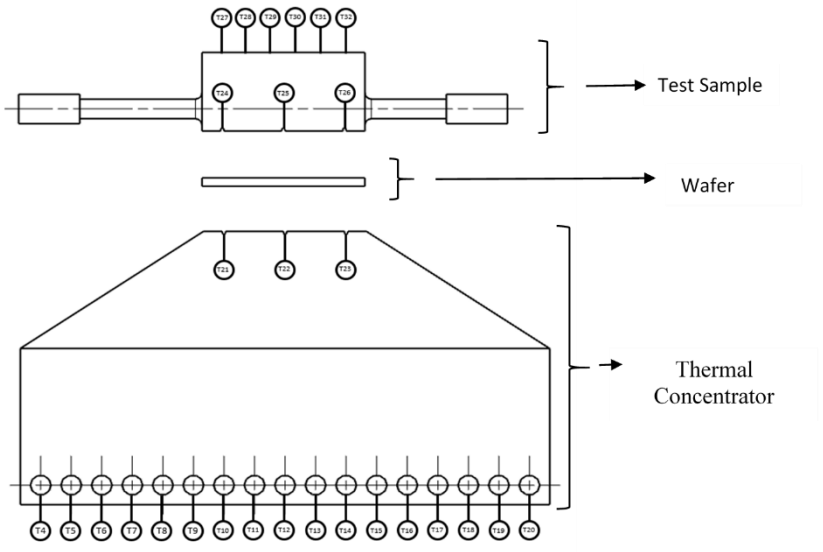

Figure 3.2: Major Components of Second-Generation High Heat Flus Test Facility

3.4 Upgraded Copper Block Design Justifications

The experimental design iteration of the second-generation high heat flux test facility's heating block is based on a series of finite element analyses simulations that allowed for a clear comparison of heat distribution yielded by different block geometries and heater placement/configuration. Using ANSYS Workbench 11.0, steady state thermal simulations were performed on the high heat flux test facility to observe the heat's motion through the trapezoidal portion of the block and into the channel. This study clearly demonstrates that the test article (channel) will be heated to the desired temperature and that there are no heat concentration regions around the heater slots that could potentially cause the heaters to overheat. The presented work focuses on the chosen configuration for the second-generation high heat flux test facility and it uses boundary conditions that were mathematically derived from previous experimental trials.

3.4.1 System Heat Input Boundary Conditions

A major driver for this experiment is the rate of heat transfer into the working fluid. As already mentioned, gasification of the cryogenic working fluid is highly possible if more than

enough heat is applied to the cooling channel. This gasification phenomena could result problematic in the analysis of the experimental data due to the lack of mathematical models to analyze two-phase flow. In order to mitigate this, a pressure drop analysis was done on the second-generation high heat flux test facility system using the maximum flow rate (0.06 kg/s) experienced in previous experimentation trials done on the first-generation high heat flux test facility. The purpose of this analysis was to attain the maximum amount of heat that could be absorbed by the liquid cryogenic at a given flow rate before actually gasifying. In carrying out this analysis, it was found that at the maximum experimental flow rate (0.06 kg/s), the cryogenic would be able to absorb a maximum of 7,225 W before gasifying. Hence, the second-generation high heat flux test facility required heaters that would be able to deliver a total of 7,225 W of heat (i.e. inlet boundary condition). Figure 3.3 illustrates the inlet boundary conditions used for the thermal simulation.

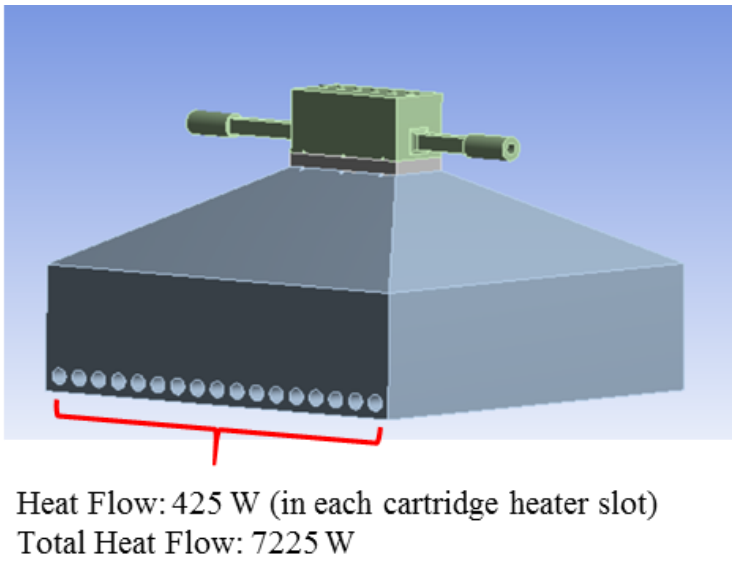

Figure 3.3: Thermal Simulation Inlet Boundary Conditions

3.4.2 System Heat Output Boundary Conditions

Since one of the goals of this study is to validate experimental repeatability, it is important for certain parameters to remain in accordance with previous experimentation trials. Hence, in

order to apply a reasonable output boundary condition, a convection heat transfer coefficient was calculated based on previous data. The convection model applied assumed this to be a perfect system, meaning that all 7,225 W of heat input would be outputted through internal forced convection by the cryogenic working fluid. Furthermore, this model also assumed that the maximum temperature reached by the test article was approximately 275 °C at the maximum flow rate of 0.06 kg/s. The film temperature used for the analysis was that of the cryogenic fluid prior to entering the test section, and any losses due to convection/radiation were neglected since the facility is under vacuum. In carrying out this analysis, it was found that the appropriate convective heat transfer coefficient to apply to the four walls of the channel was 28,508 W/m^{2}K. This coefficient would ultimate yield the desired temperature at top of the wafer and allow for close inspection of temperature gradients on different sections of the high heat flux test facility. Figure 3.4 shows a schematic of the outlet boundary conditions applied on this study.

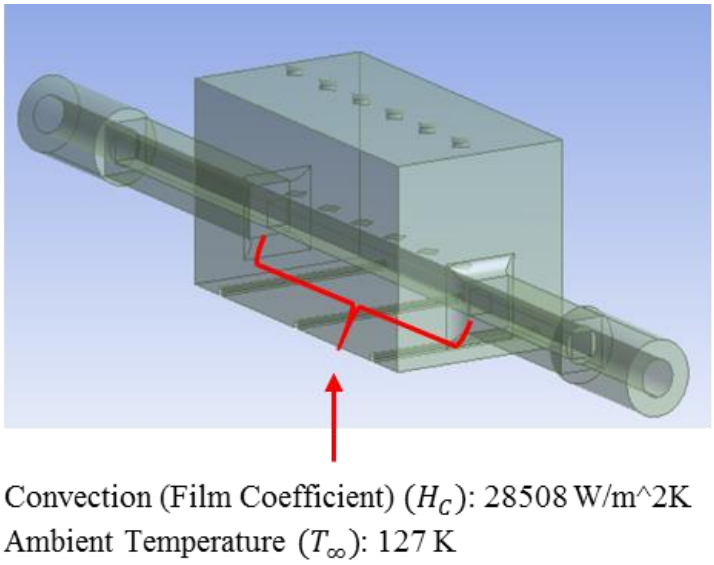

Figure 3.4: Thermal Simulation Outlet Boundary Conditions

3.4.3 Heater Configuration

The heater configuration for this design was chosen on the basis of the results attained from the thermal simulations conducted. A very important parameter to consider when dealing with electrically resistive cartridge heaters, is their watt density relative to their maximum allowable watt density. The watt density of a cartridge heater can be calculated using its geometric parameters and power rating, while its maximum allowable density is a function of hole fit (tolerance) and maximum temperature seen by the sheath of the heater, as shown in Figure 3.5. The main goal, when selecting a cartridge heater configuration, is to ensure that its watt density does not exceed its maximum allowable watt density. Whilst, the simulations were ran with the purpose of providing the temperature seen by the sheath of heaters so that the maximum allowable watt density could be attained. A fit of 0.002" was assumed, since this is the fit recommended by the heater manufacturer.

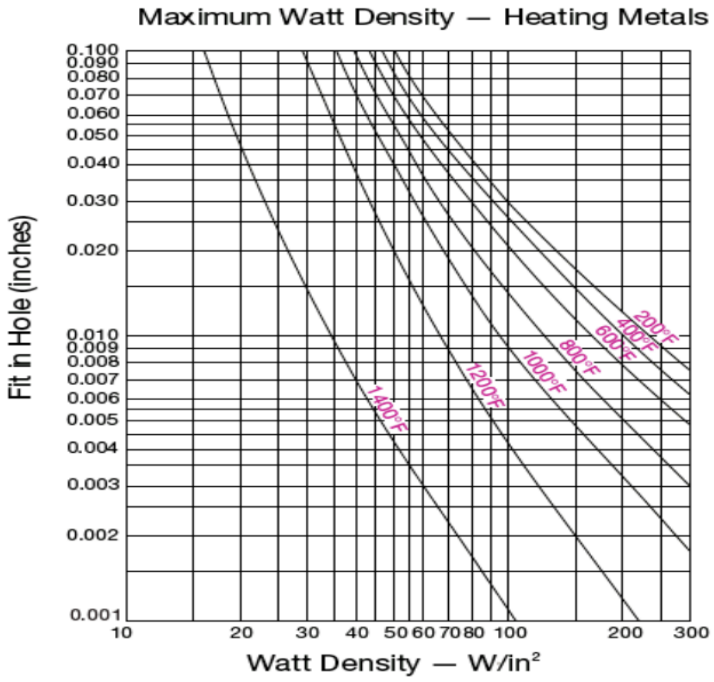

Figure 3.5: Cartridge Heater Watt Density-Fit in Hole Curve

3.4.4 Final Block Design

After simulating several block geometries and heater configurations, the shape of choice was a short-wide block with the heater slot arrangement set as a single bottom row, as illustrated by the technical drawing in the Appendix. The single bottom row demonstrated to have the lowest temperature at the heater interface which is required to assure the survival of the cartridge heaters from excessive heat. The temperature was about 980 °F (800 K), as seen in Figure 3.6, which is within the operational limit of the heaters. The heaters of choice were ¼" OD, 425 W heaters to allow better heat adjustability when turning them on and off. Furthermore, this heater configuration allowed for a higher watt density, which in turn made the heaters more resistant to higher temperatures. Moreover, the results in Figure 3.7 clearly demonstrate that the incorporation of the aluminum wafer between the heating block and test sample, will in fact provide a large enough thermal resistance to measure the heat going into the sample. The delta T across the wafer is approximately ~130 K and it is concluded that the change in temperature is evenly distributed along a flat plate.

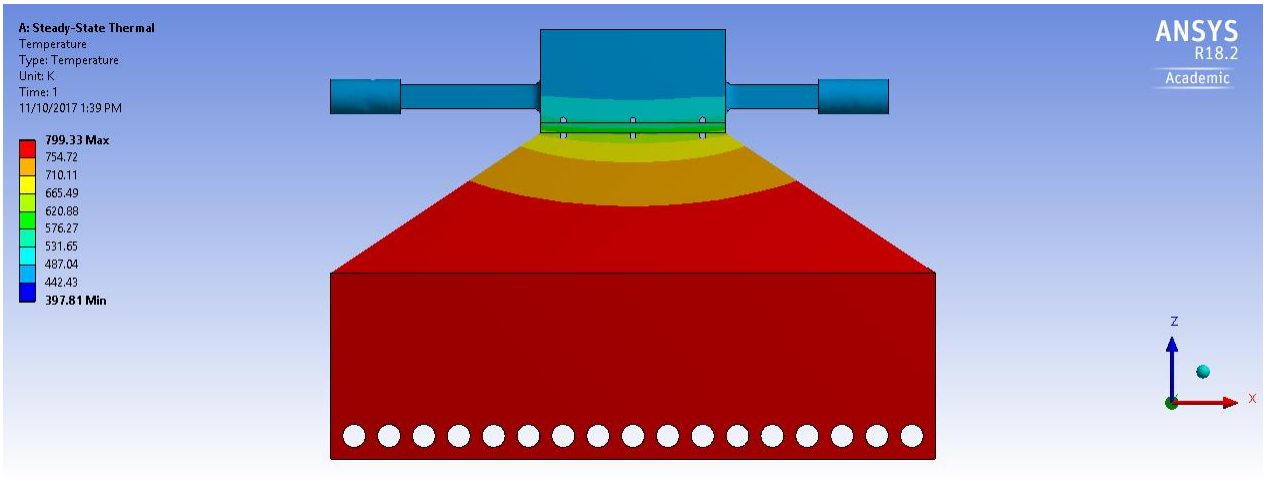

Figure 3.6: Temperature Concentration at Heater Locations

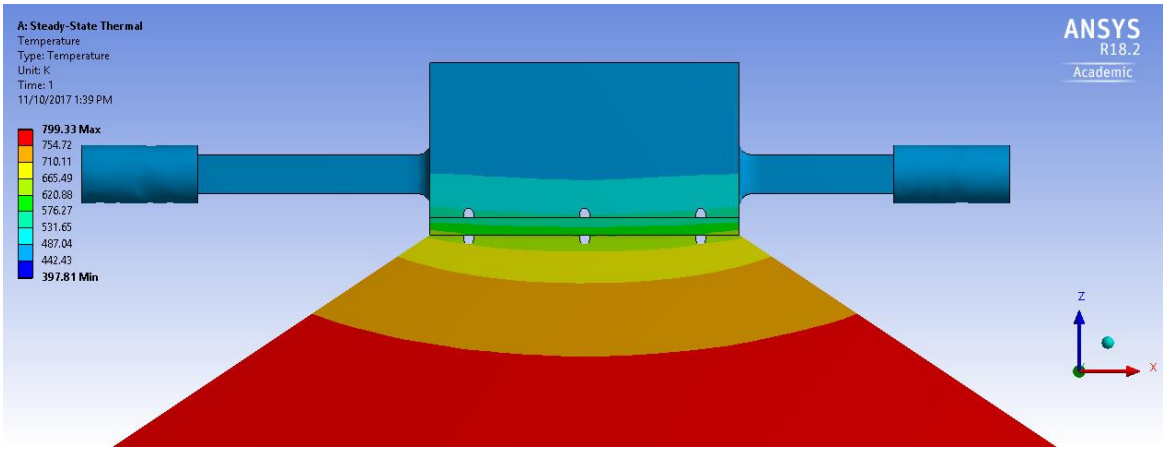

Figure 3.7: Temperature Difference Across Aluminum Wafer

3.5 Complete List of Components for Second-Generation High Heat Flux Test Facility

The components that make up the HHFTF assembly include an already assembled 316L stainless steel test stand, a newly designed heating block made of C12200 copper with 17 slots on its sides to accommodate heating cartridges (refer to technical drawing in Appendix), a thin (0.2”) aluminum wafer sandwiched in between the heating block and cooling channel, a cradle made of 6061-Al, and Inconel 625 test sections, as well as one C18200 copper section tested for data comparison with previous experimental trials. Grooves were machined on top of the heating block and on the bottom of the test sections in order to accommodate thermocouples for real time temperature measurements across the wafer. Figure 3.8 shows components.

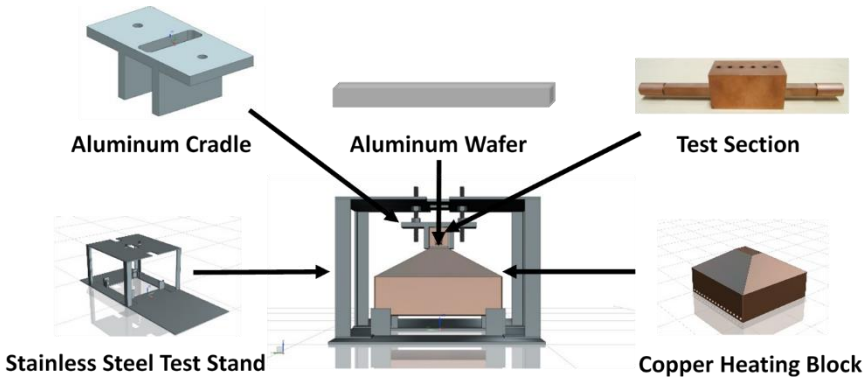

Figure 3.8: High Heat Flux Test Facility Experimental Set-Up Assembly

3.5.1 Copper Heating Block

The concept of the newly designed heating block is an adaptation of the Airforce's High Heat Flux Facility described in [9, 12, 13, and 14], as well as the first generation High Heat Flux Test Facility design by the Center for Space Exploration and Technology Research at the University of Texas at El Paso [11]. The dimensions of the newly designed heating block are 6.5" x 6.5" x 3.5" (16.5 cm x 16.5 cm x 8.9 cm) with a 45°-angled tapered section at the top designed to geometrically focus the conducted heat onto a 1" x 2" (2.5 cm x 5.1 cm) surface, as illustrated by the technical drawing in the Appendix. A total of 17 holes of 0.25" (0.635 cm) in diameter were machined on the side of the block symmetrically spaced on a single row 0.5" (1.25 cm) from the bottom of the block. These holes serve the purpose of accommodating the heating cartridges, which are the system's heat source. Copper was chosen as the heating block's material because it has a thermal conductivity of 365 W/m-K and a working temperature of 760 °C.

A major concern with the heating block, were the radiative heat transfer losses it would undergo once the mass was heated to the desired temperatures. Hence, in order to mitigate this, the block was assumed to be placed under vacuum and a preliminary assessment was conducted to calculate the radiative heat transfer losses. It was discovered that at the maximum temperature, set forth by the test matrix, the block would undergo an insignificant 1.8% radiation loss. Whilst, it was concluded that testing under a vacuum environment would provide the experiment with insignificant radiation heat transfer losses.

3.5.2 Aluminum Wafer

An aluminum T-6061 wafer was incorporated in between the heating block and the test sample. The dimensions of the wafer are 1" x 2" x 0.25" (2.5 cm x 5.1 cm x 0.635 cm), to provide an exact fit with the top surface of the heating block and a large enough thermal resistance to

measure the heat input going into the channel. It is expected that the aluminum's small thermal conductivity (167 W/m-K), relative to copper (365 W/m-K), will provide a large enough temperature difference (delta T) across the wafer, which will in turn make it simple to quantify the heat flux going into the channel through a simple thermal resistance analysis. Temperature measurements will be taken through the thermocouples placed inside the grooves machined on top of the heating block and on the bottom of the channels.

3.5.3 Test Stand for Second-Generation High Heat Flux Test Facility

The HHFTF is supported by an already assembled stainless steel 304 L stand as shown in Figure 3.9. The stand supports the four bottom corners of the heating block using small plates welded onto the L-shaped brackets, without obstructing the heater ports. Furthermore, these small plates make direct contact with the heating block and therefore was covered with Unifrax 1600 High Temperature Paper Insulation (thickness 0.0394") prior to mounting the block on the stand, in order to reduce heat transfer losses due to conduction. A square slot was machined at the bottom of the stand to allow for system wiring as needed, and the two blots/screws at top of the stand are used to interface the stand with the aluminum cradle. This stand is capable of supporting the total weight of the HHFTF, which is approximately 15 kg.

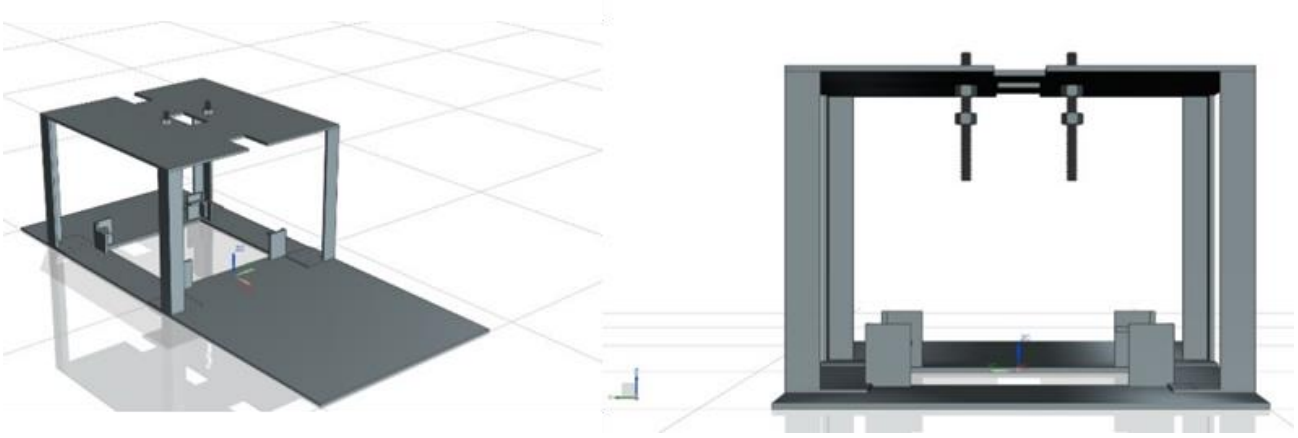

Figure 3.9: Test Stand for High Heat Flux Test Facility

3.5.4 Cradle

The function of the cradle shown in Figure 3.10, is to allow for firm contact between the test sample and the heating block. Aluminum T-6061 was chosen as the material for this component due to the cost of machinability in comparison to stainless steel. Very much like the small welded plates on the test stand, the area making contact with the test sample was also be covered with Unifrax 1600 High Temperature Paper Insulation (thickness 0.0394") prior to the placing of the cradle on top of the test sample to reduce heat transfer losses due to conduction. Once the HHFTF assembly (i.e. block, wafer, test sample, and insulation) is mounted on the test stand, the cradle will be placed on top of the test sample. The bolts will then be tightened to add pressure between the test sample and heating block, providing a good interface (firm contact) so that the heat is conducted effectively onto the channel. Thermocouples will be placed through the slot machined on top of the cradle to measure the temperature across the length of the channel.

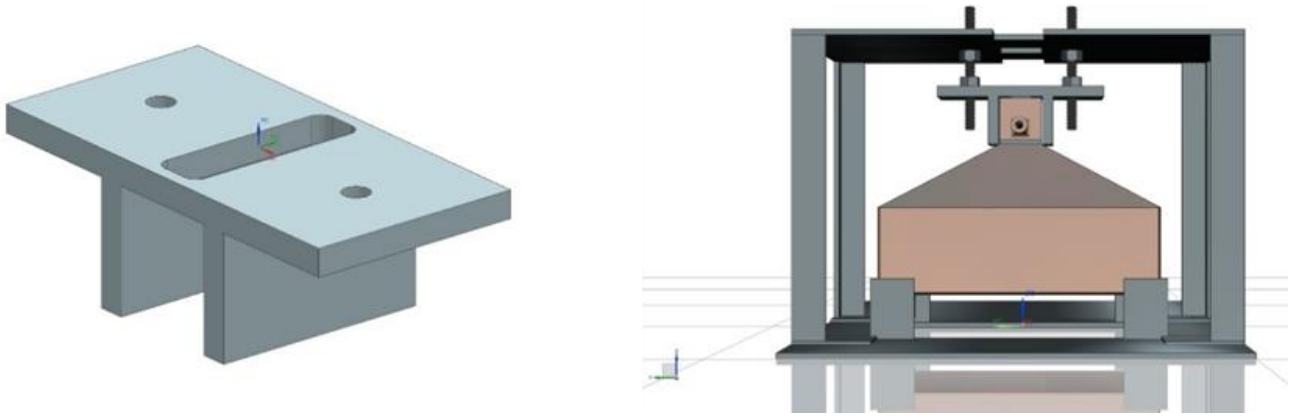

Figure 3.10: Cradle Pressure-Down Mechanism on High Heat Flux Test Facility

3.5.5 Test Section Cooling Channels

Previous tests at the Center for Space Exploration Technology Research have used C18200 copper as its test section. Copper is the industry standard for cooling channel wall material due to its high thermal conductivity [15]. In this study however, only one copper test section is tested for

the sake of comparing data to previous experiments and validating the newly designed experimental set-up. The remaining three test sections were chosen to be made out of Inconel 625 since Inconel alloys are commonly used in rocket engine design, as they are able to withstand large mechanical stresses and strains while being exposed to high temperatures.

In addition to channels being made of different materials, typical milled cooling channels in a regenerative cooled rocket engine may also vary in cross-sectional geometry throughout the engine's contour. Whilst, the HHFTF was developed such that different test section cooling channels can be easily substituted within the setup. The test section consists of a calculated entry length, a heated section, and an exit length. The entry length was designed to allow the fluid to become fully turbulent before entering the heated section. Once the fluid enters the heated section of the cooling channel, its temperature profile along the length of the test section is recorded by six axially placed type-E thermocouples. These thermocouples do not disrupt the flow since they are not in direct contact with the fluid. Instead, there exists a very small wall thickness (1.27 mm) separating the tip of thermocouple from the fluid. In addition, two wetted type-E thermocouples are used at the inlet and outlet of the cooling channel test section to record the bulk fluid temperature. Lastly, grooves at the bottom of the cooling channel are machined in order to accommodate thermocouples for temperature measurements at top of the aluminum wafer. The purpose behind attaining these measurements will be later explained under the theoretical approach section. Figure 3.11 illustrates the test section with its thermocouple arrangement.

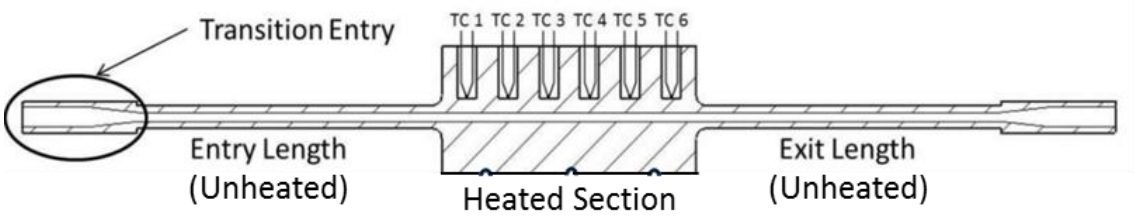

Figure 3.11: Test Section Schematic. Entry Cross Section Will be Squared at 3.2 x 3.2 mm.

This study tests five different test channels, all possessing a square cross-section of 3.2 x 3.2 mm. The test section used for comparison with previous data, is made of copper C12800 and has a surface finish of 0.8 μm. Three additional Inconel 625 test sections were traditionally manufactured and have roughened channels with surface finishes of 0.8, 3.2, and 6.4 μm. The final fifth test section was additively manufactured out of Inconel 625 and has a roughened channel with surface finish of 12.5 μm. All roughness measurements are based on the arithmetic mean value scale (Ra scale). The purpose of the selected test sections is to study the effects of surface roughness on cooling effectiveness. Moreover, this study will also aim at providing a comparison between traditionally manufactured and additively manufactured channels. This is a unique incentive behind the research being conducted because cooling channels are generally too small and abstract in geometry, to the point that traditional manufacturing methods are simply not adequate to yield the desired geometric parameters. Hence, by experimenting with additively manufactured channels, it is possible to assess the impact of the manufacturing process on the channels surface roughness and relating results to the channel's overall cooling effectiveness. This in turn, could potentially signify the feasibility in presenting additive manufacturing as a more cost/time effective alternative for producing regenerative cooled rocket engines in the future.

Chapter 4: System Measurement Instrumentation and Components

4.1. System Measurements

Instrumentation incorporated in the HHFTF is used to measure three driving parameters for this study; temperature, pressure, and flow rate. All instrumentation was verified to possess the capability of operating at the required conditions as set forth by this study. The system's operable temperatures, pressures, and vacuum levels are 650 °C, 1.5 MPa, and 2.5 x 10^2 torr respectively. In addition, a data acquisition system is integrated into the experimental set-up to acquire and record data for post-processing purposes. This instrumentation is further discussed in the following sub-sections, and a more detailed description of all instrumentation is found in the Appendix.

4.1.1. Temperature Measurements

Temperature monitoring of the copper heating block was done through the use of 17 type K thermocouples (provided by Dalton Electric) each accommodated on grooves already manufactured on the heating cartridges. Additionally, six exposed tip type E thermocouples were used to measure the wall temperatures throughout the length of the test section. Furthermore, a total of six exposed tip type E thermocouples (0.05" thickness) were placed on the grooves machined on top of the heating block and bottom of the test section to measure the temperature gradient across the wafer, and two ungrounded sheathed (304 SS, 3.0 mm sheath) type-E thermocouples were utilized to measure the fluid bulk temperatures. Figure 4.1 provides a visual of all thermocouples used within the experimental set-up.

Figure 4.1: Dalton Electric Type K Thermocouples (left) and Omega Ungrounded Sheathed Type E Thermocouples (right)

4.1.2. Pressure Measurements

Two thin-film cryogenic pressure transducers (Omega PX1005L1-500AV) were placed at the inlet and outlet of the channel to measure pressure drop across the channel. These pressure transducers also provide the pressure measurements needed to calculate the experimental bulk pressures used to attain the fluid's properties. Furthermore, another pressure transducer was placed downstream of the LN_2 in order to monitor the fluid pressure coming out of the dewar. In addition, vacuum levels inside of the vacuum chamber are measured through the use of a pirani gauge controller and a convection-enhanced pirani sensor. Figure 4.2 illustrates all devices used for pressure measurements.

Figure 4.2: (a) Omegadyne Thin Film Cryogenic Pressure Transducer (b) Pirani Vacuum Gauge Controller (c) Convection-Enhanced Pirani Sensor

4.1.3. Mass Flow Rate Measurement

A turbine flowmeter (Hoffer HO1/2X1/4A Series), is installed in the propellant line, upstream of the test section. Because the flow meter's rpm depends on the fluid's density and velocity, the flow meter was calibrated to be used with LN_2 prior to experimentation. The flow meter is rated to a range between 0 and 17 Liters per minute. Figure 4.3 shows a visual of the flow meter used in this study.

Figure 4.3: Flow Meter Hoffer HO1/2X1/4A Series.

4.1.4. Data Acquisition System

A data acquisition system (DAQ system) is utilized to record all data points throughout the duration of the test. Two NI 9213 USB input modules are used for temperature measurements, and an NI SCC-68 unit coupled with an NI PCI-6533 is used for pressure and mass flow rate measurements. In addition, both pressure transducers are connected to a 1/8 DIN process meter and controller for signal conditioning. This is convenient because it allows the display to be seen by the personnel monitoring the system's pressures. All data is recorded with a sample rate of 10 Hz. Figure 4.4 shows a visual of the instrumentation that makes up the data acquisition system.

Figure 4.4: NI PCI-6533, NI SCC-68, NI 9213 and Omega 1/8 DIN Process Meter.

In addition, a graphical user interface (GUI) was created to view some real-time output signals based on the data collected by the DAQ system, as shown in Figure 4.5. The GUI shows the block temperatures at each cartridge heater slot, temperatures at the top and bottom of the wafer, test section wall temperatures, as well as channel inlet and outlet temperatures and pressures. The "record" switch is activated once the system reaches the block temperatures established on the test matrix.

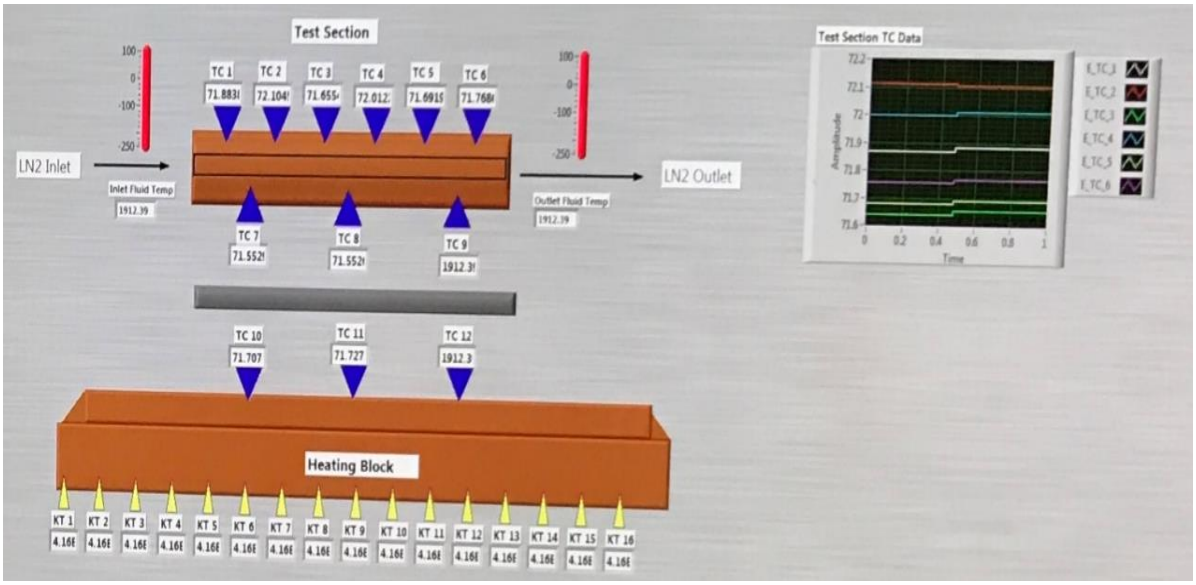

Figure 4.5: NI LabVIEW 13.0 HHFTF Graphical User Interface

4.2. Line Components

A Piping and Instrumentation Diagram (P&ID) was generated to assist with assembling the experimental set-up and following the test procedure, Figure 4.6. As evident by the P&ID, the experimental set-up incorporates several different components that serve different functions such as regulating back pressure, and controlling the flow path of the fluids used in the experiment. The following sub-sections further discuss the specific line components used in this study.

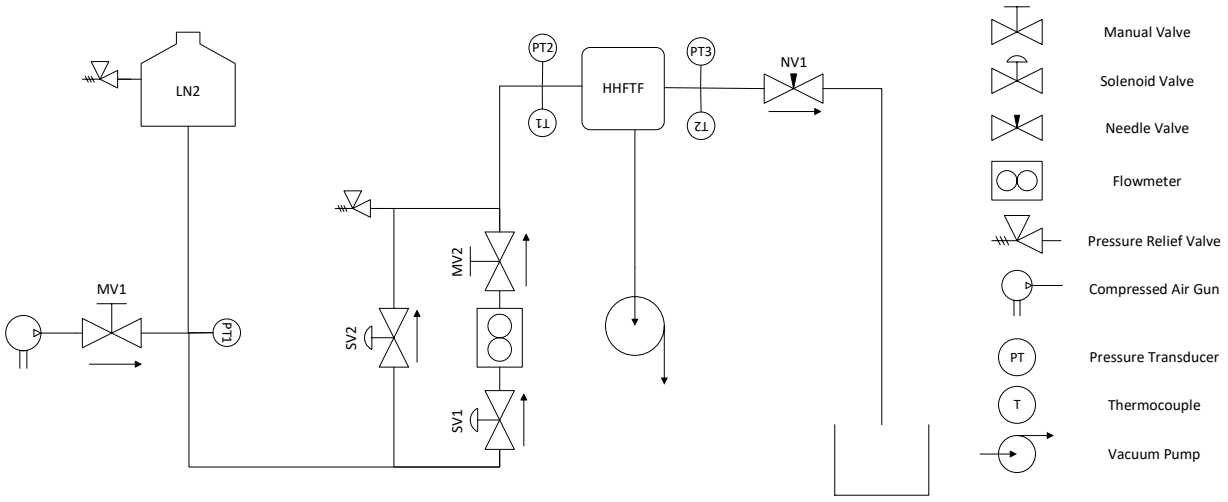

Figure 4.6: Piping and Instrumentation Diagram for HHFTF Experimental Set-Up

4.2.1. Manual Valves

The system incorporates two short stem globe manual valves made of brass as shown in Figure 4.7. These valves are rated for cryogenic flow and manufactured by Rego Products. The manual valves are mainly used for pre-testing procedures such as purging and pre-chilling. Both valves are used to control flow when executing these procedures, in order to properly ensure that the system does not overchill prior to beginning a test, as well as ensure that no gas during the purging procedure reaches and over-spins the flowmeter.

Figure 4.7: Rego Products' Cryogenic Manual Valve

4.2.2. Solenoid Valves

The actuated valves used in the system, are cryogen rated Gems Sensor and Controls "D-Cryo Series Solenoid Valves," Figure 4.8. Two of these valves are used in the line system to supply LN_2 to the flowmeter when pre-chilling, and to the channel during an actual test. These valves are used to control flow in time spans shorter than tenths of a second. The power requirement for these valves is 12 V at 1.2 A. Valve control will be discussed in the following section.

Figure 4.8: Gem Sensor and Controls' Cryogenic Solenoid Valve

4.2.3. Needle Valve

The needle valve used for LN_2 flow control is a cryogen rated 316 SS valve made by Dragon Valves Inc, Figure 4.9. This valve is placed downstream of the channel to provide back pressure and thus allow for adequate control of LN_2 flow rate passing through the channel. Furthermore, this valve also provides a system seal when being evacuated.

Figure 4.9: Dragon Valves Inc's Cryogenic Needle Valve

4.2.4. Pressure Relief Valves

Since the working fluid for this study is liquid nitrogen, gasification and over-pressurization within the system lines is a prominent concern. As a way to mitigate this, relief valves have been placed at critical points where the cryogenic fluid is more like to be trapped and eventually gasify creating pressure. These valves activate at 2.4 MPa. Both Swagelok pressure relief valves used are cryogen rated and can be seen on Figure 4.10.

Figure 4.10: Swagelok's Cryogen Rated Pressure Relief Valve

4.2.5. Line Vacuum Pump

Safety concerns require that air be evacuated from all propellant lines prior to beginning any test in order to prevent moisture in the air from freezing inside the line. In addition, and more specific to this study, dissimilar channel surfaces for each test are a possibility because the copper is heated to high temperatures such that an oxidation layer may form inside of the channel walls. Hence, pulling vacuum inside of the lines prior to every test can mitigate this possible issue by ridding the system of this layer. A piston powered vacuum pump is used to pull vacuum inside of the lines. This vacuum is interchangeable with the compressed air gun found on the P&ID, as per

the test procedure. Typical line vacuum levels are 6.9 kPa. Figure 4.11 shows the vacuum pump used for this procedure.

Figure 4.11: Rocker 300 Vacuum Pump

4.2.6. Chamber Vacuum Pump

In addition to pulling vacuum inside of the lines, vacuum is also pulled in the chamber to approximately 6.7 Pa (5.0 x 10^{-2} torr) to reduce convective losses of the system. Moreover, this is also done to prevent the heating block from experiencing oxidation, since oxidation on the contact surfaces between the block and the test section would affect the heat transfer between the two surfaces. The pump used for this procedure is shown n Figure 4.12.

Figure 4.12: Edwards XDS5 Scroll Vacuum Pump

4.3. Electrical Components

The electrical components utilized in this set-up include the two solenoid valves previously discussed, the three pressure transducers also previously discussed, and 17 cartridge heaters. Two Extech Quad Output DC power supplies (Figure 4.13) connected to standard 120 VAC power outlets are used to power these components in order to be able to adjust the voltage and current levels that are required to operate the actuated solenoid valves and pressure transducers. The valves require a voltage level of 12 VDC and draw approximately 1.3 A, while the pressure transducers are activated by an excitation voltage of 10 VDC.

Figure 4.13: Extech Quad Output DC Power Supply

4.3.1. Cartridge Heaters

The cartridge heaters used to supply heat to the block are 425 W-120 VAC heaters manufactured by Dalton Electric, Figure 4.14 (a). These heaters are controlled by a series of solid state relays (SSR) interfaced as shown on the wiring schematic illustrated by Figure 4.15. A total of three heaters are connected per solid state relay (with one SSR having only two heaters connected to it). Each solid state relay, Figure 4.14 (b), is manually powered by a switch connected to a DC power supply of 5 VDC discussed in the previous section. This means that when each

solid state relay is triggered by their respective switch, current is allowed to flow through the three (or two) cartridge heaters connected to it. Such interface was chosen to control the heat input going into the test channel. Figure 4.14 (c) illustrates the control box that was made to control the heaters and actuated solenoid valves.

Figure 4.14: Dalton Electric Cartridge Heaters and Solid-State Relay

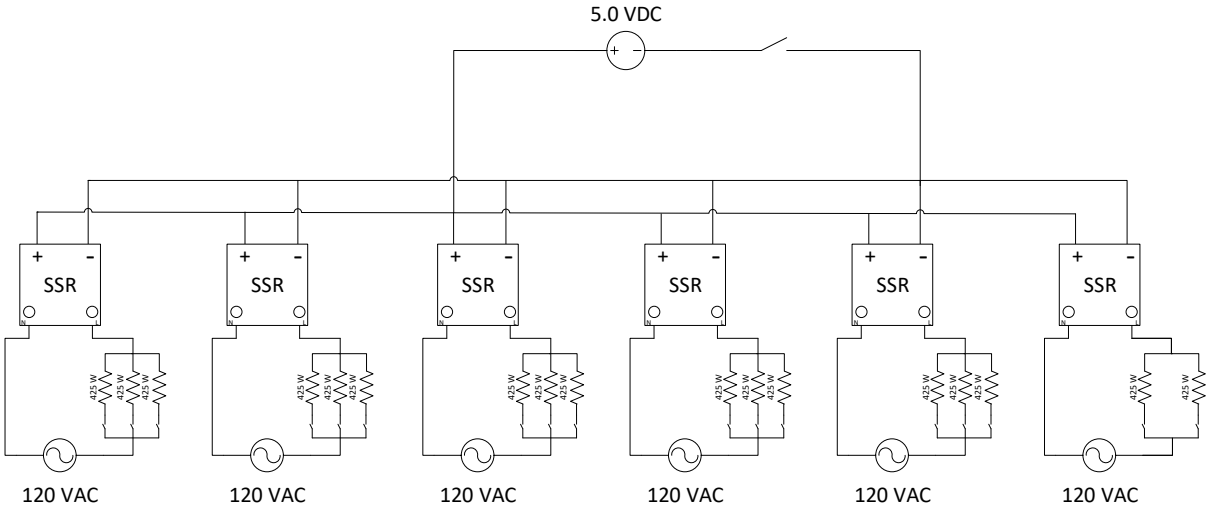

Figure 4.15: Cartridge Heater Wiring System Schematic

Chapter 5: Experimental Methodology

5.1. Test Procedure

The test procedure is divided into three major components; pre-experimental procedure, experimental procedure, and post-experimental procedure. The pre-experimental procedure focuses on the preparation of the system lines and instrumentation. The experimental procedure, on the other hand, details the process for heating the block, flowing LN_2 through the test section, and recording all data. Lastly, the post-experimental procedure outlines the processes followed to safely shut off all systems. The following sections give a brief overview of the entire experimental procedure and a more detail procedure, along with an emergency procedure with red lines and risk/hazards, is included in the Appendix.

5.1.1. Pre-Experimental Procedure

Prior to beginning the experiment, all instrumentation, including thermocouples, pressure transducers, heating cartridges, actuated valves, manual valves, and power supply units are inspected to ensure their proper functionality. Furthermore, all personnel are equipped with proper cryogenic personal protective equipment (PPE) to protect against liquid nitrogen (LN_2), which will be the working fluid for this study. At this point, vacuum is pulled in the system lines to prevent moisture in the air from freezing inside the line. Pulling vacuum also removes any additional fluid residuals which may be present inside the lines from previous experiments. In addition, vacuum is also pulled in the chamber to approximately 6.7 Pa (5.0×10^{-2} torr) to reduce convective losses of the system.

5.1.2. Experimental Procedure

After preparation of the system, the heating process begins by turning on the heaters and heating up the block to the temperatures stated on the test matrix. Unlike previous generations of

the high heat flux test facility, this setup iteration incorporates a thermocouple on each cartridge heater that serves the purpose of monitoring the heater's temperature real time in order to avoid failure. Each cartridge heater is rated to 480 °C, therefore any temperature reading above 350 °C would require an immediate shut off of the heaters.

Once the block reaches the specified conditions in the test matrix, the delivery line and test section are pre-chilled by beginning the flow of LN_2. As the lines are being pre-chilled, the needle valve downstream of the cooling channel is adjusted while the flowmeter is monitored to read the mass flow rate required by the test matrix. Once the mass flow rate is set and the test section channel inlet conditions reach the parameters established on the test matrix, the data acquisition system is initiated. The test ends once the temperature readings on top of the cooling channel stay within 1 ºF from each other for each thermocouple for at least 20 seconds. This signifies that enough steady state data has been collected and the LN_2 flow may be subsided.

5.1.3. Post-Experimental Procedure

Post- experimental procedure dictates that all system valves be opened to ventilate the remaining cryogen in the lines. Furthermore, cleaning of surfaces on the heating block and test channel is done as needed, so as to prevent oxidation build up. Lastly, the integrity of the heaters and thermocouples is tested to assure their proper functionality. A voltmeter is used to measure the resistance of each cartridge heater, while the temperature reading of each thermocouple is monitored until it reaches ambient temperature (~25 °C).

5.2. Theoretical Approach

In this study, there are two modes of heat transfer; conduction and convection. The conduction heat transfer refers to the heat input being conducted from the heaters onto the test section, while the convection heat transfer refers to the actual heat being removed from the test

section and absorbed by the working cryogenic fluid LN_2. The following sections explain how both modes of heat transfer were analyzed and quantified. It is important to note that the convection heat transfer was the one utilized for the Reynolds and Nusselt numbers plot later discussed. Although this equation is only valid for convective heat transfer, in this case it is used as an approximation of the actual heat fluxes of the film-boiling data.

5.2.1. Conductive Heat Transfer

A major driver for this experiment is the rate of heat transfer going into the test section cooling channel. Because the thermal concentrator (block) used to deliver heat into the test sample possesses a relatively abstract geometry, a method was designed to measure this particular heat flux. This method consists of inserting a small piece of rectangular aluminum wafer between the block and the test sample as shown in the Figure 5.1. The aluminum's small thermal conductivity, relative to copper, will create a thermal resistance and provide a large temperature difference ΔT across the wafer, which will in turn make it simple to quantify the heat flux going into the test sample by using Eq. (5.1). Figure 5.2 shows the trend relating the system's heat input to the temperature difference across the aluminum wafer.

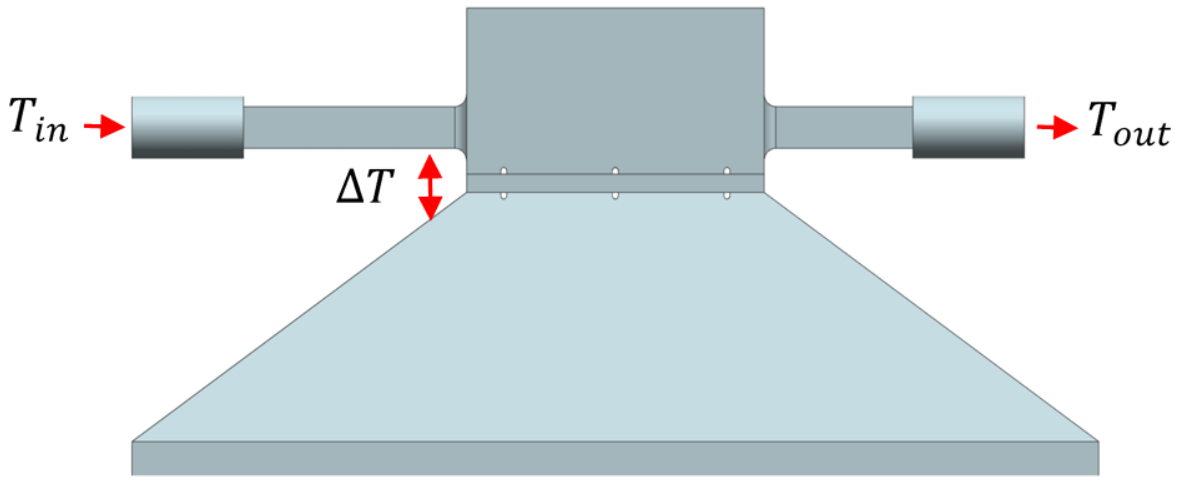

Figure 5.1: Aluminum Wafer Placement on High Heat Flux Test Facility

$$Q_{in} = \frac{k\Delta T}{t} A \tag{5.1}$$

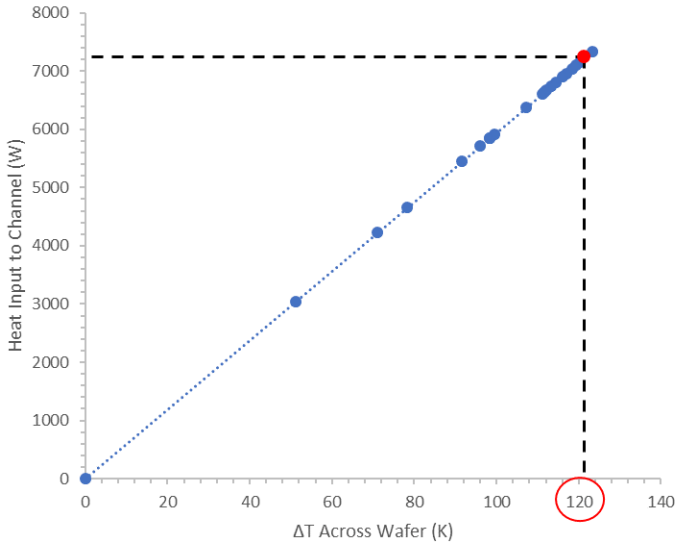

Figure 5.2: Channel Heat Input as a Function of Temperature Difference Across Wafer

5.2.2. Convective Heat Transfer

Another very important parameter to consider in this study, is the rate of heat transfer to the fluid. This was calculated using a basic heat transfer equation based on the mass flow rate of the fluid $\dot{m}$, specific heat C_p, and temperature differential from the channel's inlet to outlet ΔT, as remarked in Eq. (5.2) [12]. Furthermore, heat flux q'', was determined by using the test section coolant channel's wetted wall surface area A_w, as depicted in Eq. (5.3).

$$Q = \dot{m} C_p (T_{out} - T_{in}) \tag{5.2}$$

$$q'' = \frac{Q}{A_w} \tag{5.3}$$

As stated before, mass flow rate was attained from the flowmeter readings throughout the duration of the test. After having adjusted the needle valve downstream of the channel to the appropriate position, the mass flow rate readings proved to be steady, deviating only by ±0.005 kg/s from the test matrix parameters. No issues such as overspinning were ever experienced in any of the experimental trials. The convection coefficient h was then calculated using Eq. (5.4) by using the heat flux resulting from Eq. (5.3), the average wall temperature T_w, and the average bulk temperature $T_b = ½(T_{in}+T_{out})$.

$$h = \frac{q''}{(T_w - T_b)} \tag{5.4}$$

Lastly, the measured results were used to develop correlations for Nusselt and Reynolds numbers. Nusselt number Nu_D is defined as the ratio of the convection coefficient to the fluid conduction coefficient k at the test article's specified hydraulic diameter $D_{hyd,}$ as shown in Eq. (5.5). Moreover, Reynolds number is defined by Eq. (5.6) using the fluid density ρ, fluid viscosity μ, test article hydraulic diameter D_{hyd}, and bulk velocity υ calculated from the $\dot{m}$, ρ, and coolant channel cross-sectional area.

$$Nu_D = \frac{h}{k} D_{hyd} \tag{5.5}$$

$$Re = \frac{\rho \upsilon D_{hyd}}{\mu} \tag{5.6}$$

All state properties ρ, μ, C_p, and k, were calculated using REFPROP [11] at the average fluid pressure P_{av}, where $P_{av} = ½(P_{in}+P_{out})$, and T_b.

5.3. Measurement Uncertainty Analysis

All data points collected in this study possess a maximum uncertainty primarily pertaining to the accuracies of the instrumentation reported by the vendors; refer to Table 1 in the Appendix. Eq. (5.7) illustrates the uncertainty propagation and it is employed as a means to calculate the combined error for each parameter in this study. This means that the error is a resulting effect of the measured parameters of mass flow rate, temperature, and pressures. In other words, the mass flow rate measurement is directly influenced by the flow meter during calibration, and the heat transfer coefficient measurement is directly influenced by the thermocouple readings associated with the channel wall and bulk fluid temperatures, as well as by the pressure transducer measurements associated with the bulk fluid pressures. Furthermore, REFPROP has an accuracy of ±0.2 % and thus, also has an effect on mass flow rate since it is the library used to evaluate all fluid state properties. Table 5.1 includes the percent error for each parameter.

$$(U_{cal}) = \sqrt{\sum \left(\frac{\delta f(Calculated)}{\delta Variable} Error_{variable} \right)^2} \tag{5.7}$$

Table 5.1: Instrumentation Measurement Accuracy

Measured Parameter	**Percent Error**
Turbine Flow Meter	±0.10
Pressure Transducers	±0.25
Thermocouples	±1.00
REFPROP (Fluid Properties)	±0.20
Pressure Differential	±0.35
Temperature Differential	±1.40
Mass Flow Rate	±1.23
Heat Transfer Coefficient	±2.42
Heat Flux	±2.64
Measured Nusselt Number	±6.20

Chapter 6: Results and Discussion

6.1. Test Matrix Development

The three variables in this study are the test sections' surface finish, block temperatures, and mass flow rate through the test section. Channel geometry stayed consistent for each test section tested so as to act as the control for the experiment. The inlet pressures were chosen accordingly to comply with the laboratory's safety regulations (max pressure of 1.5 MPa), and the inlet temperatures were chosen to be approximately -165 °C to ensure a subcooled liquid state.

6.1.1. Test Matrix for Experimental Set-Up Validation

The channel tested for this part of the study, was a copper sample with a 0.8 μm surface finish [11]. This test section is the same channel used by Trujillo [11] when conducting this same experiment with LCH_4 as the working fluid. The flow rates used for these LCH_4 tests were 0.05 kg/s and 0.053 kg/s, and both flow rates were tested at block temperatures of 200 °C and 275 °C. Since LN_2 is the working fluid for the study presented in this work, a non-dimensional number analysis was done prior to attain the necessary LN_2 mass flow rates and inlet conditions to equate the parameters yielded by LCH_4 tests. This analysis included equating the Reynolds number, measured Nusselt number, and predicted Nusselt number as per cook's correlation (later discussed) of both fluids, given the LCH_4 resulting parameters from Trujillo's [11] test, and computing the LN_2 mass flow rates and inlet properties that would yield a minimal percent error. Table 6.1 details the resulting test matrix parameters chosen for validating the upgraded experimental set-up.

Table 6.1: Test Matrix for Experimental Set-Up Validation

Test Matrix for 3.2 mm x 3.2 mm Cooling Channel (Length: 5.1 mm)		
Specimen	**Flow Rate**	**Block Temperature**
Copper 0.8 μm	0.02 kg/s	200 °C
		275 °C
	0.025 kg/s	200 °C
		275 °C

6.1.2. Test Matrix for Channel Surface Roughness Study on Inconel 626 Channels

After having validated the new experimental set-up, the next part of the study was to study the effects of surface roughness on cooling channels subjected to temperatures varying from 245ºC and 315ºC. During this study, three conventionally manufactured channels with different roughness finishes (6µm, 23µm, and 45µm) are compared to an additively manufactured channel with a roughness finish of 15µm. Since the channel cross-sectional geometry is the same on all of the test samples, it is expected that the cooling effectiveness will increase at the expense of increased pressure drops caused by the larger roughness finishes. In order to test this theory, larger flow rates than those previously used on LCH_4 were chosen, so as to better observe pressure drop across the channel. Table 6.2 details the test matrix parameters chosen for this part of the study.

Table 6.2: Test Matrix for Surface Roughness Study on Inconel 625 Channels

Test Matrix for 3.2 mm x 3.2 mm Cooling Channel (Length: 5.1 mm)		
Specimen	**Flow Rate**	**Block Temperature**
Copper 0.8 µm	0.04 kg/s	245 °C
		315 °C
	0.05 kg/s	245 °C
		315 °C
Inconel 0.8 µm	0.04 kg/s	245 °C
		315 °C
	0.05 kg/s	245 °C
		315 °C
Inconel 3.2 µm	0.04 kg/s	245 °C
		315 °C
	0.05 kg/s	245 °C
		315 °C
Inconel 6.4 µm	0.04 kg/s	245 °C
		315 °C
	0.05 kg/s	245 °C
		315 °C
3D-Printed (~10 µm)	0.04 kg/s	245 °C
		315 °C
	0.05 kg/s	245 °C
		315 °C

6.2. Results for Experimental Set-Up Validation

The first objective of this experiment was to establish a baseline to prove the validity of the upgraded experimental setup prior to beginning testing on the Inconel 625 channels. As discussed in the previous section, this baseline was based on previous LCH_4 experimental data acquired by Abraham Trujillo using a copper sample with a 0.8 μm surface finish [11]. It is important to note that only those parameters (flow rates) that were feasible were tested and below are the resulting Reynolds number and Nusselt number correlations acquired during LN2 testing with the calculated parameters from the non-dimensional number analysis (Table 2). Since each experimental data set uses a distinct working cryogenic fluid, a margin of error of 20% was deemed acceptable prior to beginning the data acquisition. As evident by both figures in Figure 6.1 and uncertainty calculations, the Reynolds number, measured Nusselt number, and predicted Nusselt number as per Cook's correlation, each have a percent error of approximately 8, 15, and 8 % respectively. Henceforth, this indicates a clear sign of repeatability between the old and new setup, though more testing with LCH_4 should be accomplished in order to further solidify this validation.

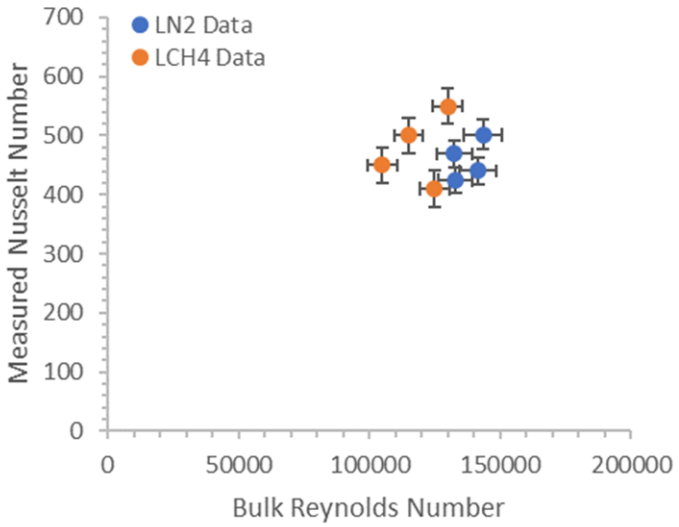

Figure 6.1(a): LN2 and LCH4 data comparison showing Nusselt number as a function of bulk Reynolds number.

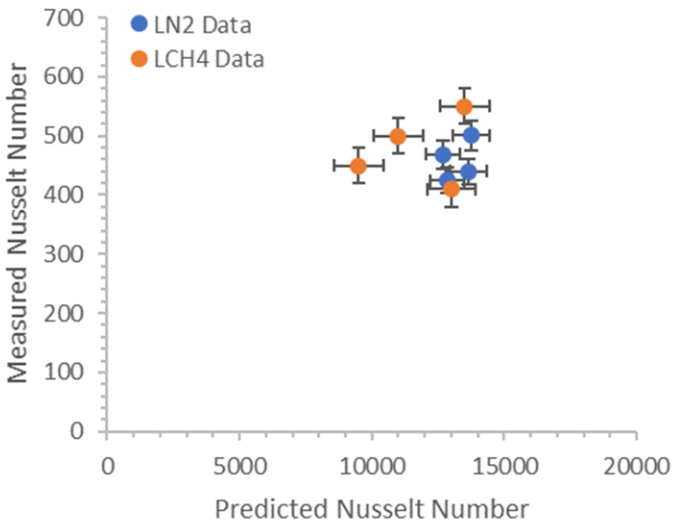

Figure 6.1(b): LN2 and LCH4 data comparison showing Nusselt number as a function of predicted Nusselt number as per Cook's correlation.

6.3. Results for Surface Roughness Study on Inconel 626 Channels

The data obtained for the Inconel 625 square channels include a total of 20 points with 4 data points per channel. One copper channel is also included on the data for the sake of comparing data from two different channel materials. All channels were tested at higher mass flow rates than those used for the LCH_4 tests discussed in the previous section. The 20 points also include the data for the additively manufactured Inconel 625 channel.

As stated before, in order for an experimental trial to be considered a success, the system must first reach steady-state. Steady-state is defined as a reasonable time interval (at least 20 seconds) during which the rate of change of the wall temperatures is approximately zero. Data points are averaged in the "steady-state" region, and Figure 6.2 shows an example of the test measurements for the six T_w thermocouples and fluid temperatures.

Through the data, it was observed that in some tests, the channel wall proved to be cooled more effectively than others. This means that the channel wall temperatures were below 0 °C.

Hence, in an effort to distinguish the different modes of heat transfer, the data was classified into three different categories: cold wall, hot wall, and mixed. Cold wall refers to the data in which all channel wall temperatures were below 0 °C; hot wall refers to the data in which all channel wall temperatures were above 0 °C; and lastly, mixed refers to the data in which both temperatures below and above 0 °C were present. The purpose in categorizing the data in such a manner, is to outline the possibility of the presence of film-boiling phenomena; that is, all "hot wall" measurements are classified as film-boiling points, and all "cold wall" measurements are classified as non-boiling points. Figure 6.2(a) illustrates an example of a "hot wall" test, and Figure 6.2(b) illustrates an example of a "cold wall" test. LN_2 was subcooled at both the inlet and outlet of the channel on all tests therefore, any film-boiling phenomena measured in the channel would be classified as "subcooled film-boiling."

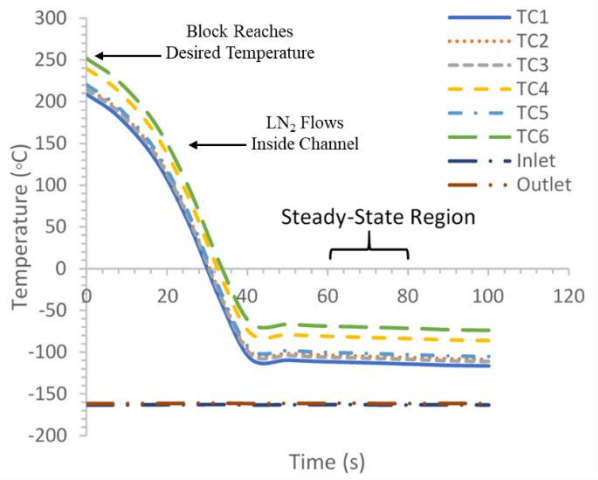

Figure 6.2(a): Cold Wall Temperature Measurements of the Six Tw Thermocouples as a Function of Time

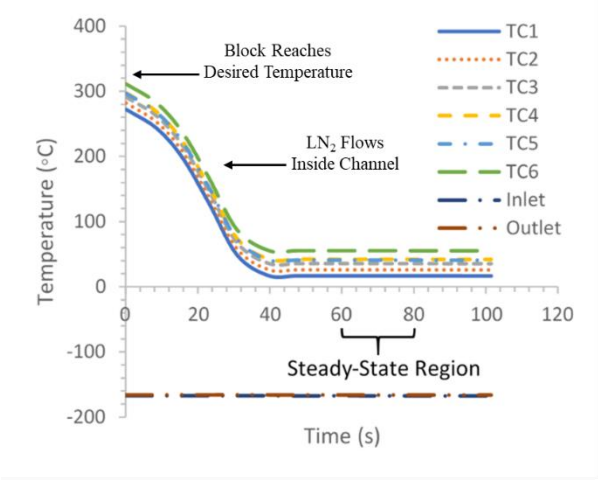

Figure 6.2(b): Hot Wall Temperature Measurements of the Six Tw Thermocouples as a Function of Time

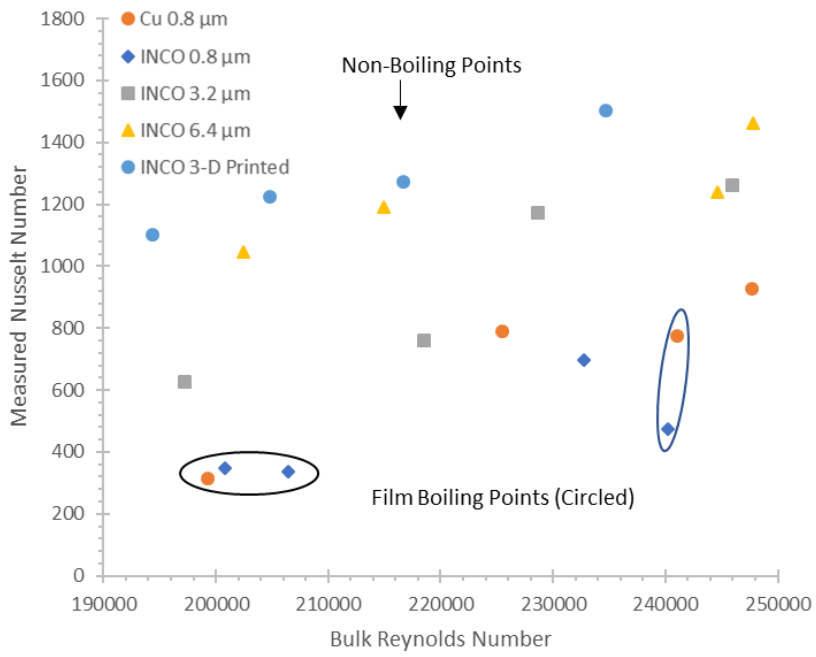

Figure 6.3: Bulk Reynolds Number as a Function of Measured Nusselt Number

Figure 6.3 illustrates the plot of the steady-state measured Nusselt number versus bulk Reynolds number, with both the film-boiling points and non-boiling points circled. This figure shows that the range of Nusselt numbers is between 350 and 1450, while the Reynolds numbers range between 195,000 and 245,000. This data compares well with the Norris correlation [16] because it shows the expected trend of increasing heat transfer with increasing surface roughness for the non-boiling points. In other words, the data can potentially support the hypothesis that the cooling effectiveness of a completely subcooled fluid flowing in cooling channels increases as channel roughness finishes increase. Thus, a preliminary deduction can be made stating that channels with additive manufactured surface finishes provide better cooling effectiveness than channels that are traditionally milled. Although this trend is evident for the non-boiling points, it is not clearly evident for the film-boiling points. Hence, more data points should be collected to better observe the effects of surface roughness on both heat transfer regimes.

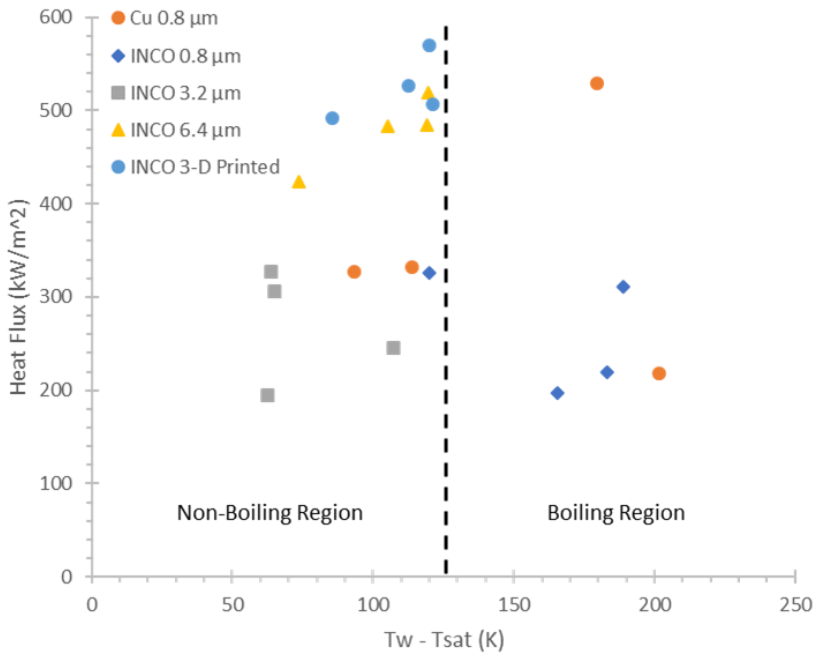

Figure 6.4: Heat Flux as a Function of Wall Temperature Minus Saturated Temperature

Illustrated by Figure 6.4 is the heat flux versus the change in temperature of the average wall temperature minus saturation temperature, where the modes of heat transfer can be more closely observed. Heat flux was calculated by using Eq. (5.2), and although this equation is only valid for convective heat transfer, in this case it is used as an approximation of the actual heat fluxes of the film-boiling data. This plot was divided into a non-boiling region and a boiling region, where it is observed that all six thermocouples in the T_w measurements read "hot" together in the film-boiling regime. This signifies that the critical heat flux (CHF) onset occurs in the 5.1 mm before the first wall thermocouple. Furthermore, it may also be deduced that the reduction in heat flux at higher wall temperatures is the result of more heat going into boiling the cryogen rather than in raising its bulk temperature. For comparison, Beduz et al., Crowley et al., and Yokouchi et al., reported CHF for LN_2 ranging from ~200 – 600 kW/m^2 [17].

In order to better observe where the critical heat flux occurs, a boiling number analysis was done to normalize the different data points for the velocities tested. The boiling number *Bo* is defined as the ratio of the critical heat flux q''_{CHF} to the LN_2 heat of vaporization i_{fg}, and mass flow per cross-sectional area A_C as shown in Eq. 7. Note that all data points were calculated at the measured q'' shown in Eq. (6.1).

$$Bo = \frac{q'' A_C}{i_{fg} \dot{m}} \tag{6.1}$$

Figure 6.5 was then generated to illustrate the boiling number versus $\Delta T(T_w - T_{sat})$, where T_{sat} represents the saturation temperature. Through this figure, it is evident that the critical heat flux occurs at a boiling number of approximately 0.056. It is then deduced that in the film-boiling regime, heat flux values are low because more heat is going into boiling rather than into raising the bulk fluid temperature. For comparison, this value of $Bo \sim 0.056$ matches well with the Shah correlation for critical heat flux in horizontal tube flow [15]. Since the year 1979, Shah has proposed a series of methods that have improved over time. Shah's most recent method (1987), includes two different correlations: the "upstream conditions correlation" (UCC) and the "local conditions correlation" (LCC). This study focuses on the "upstream conditions correlation" since the boiling number is related to a critical length of tube z_{crit} needed to reach the critical heat flux for a given amount of subcooling (i.e., negative quality x) in the upstream conditions [6]. Although other parameters are considered in the Shah correlation, the boiling number prediction is simplified in order to focus on the most important factors; (z_{crit}/D_{hyd}) and $(1 - x)$. In this study, the points around the measured critical heat flux had a subcooled quality ranging from $x \sim -0.31$ to -0.37. Furthermore, since it is assumed that the critical heat flux occurs prior to the position of the first

wall thermocouple, (z_{crit}/D_{hyd}) ~ 2. Hence, through inspection of the Shah "upstream conditions correlation" [15], the predicted boiling number for the qualities discussed would be *Bo* ~ 0.06. In order to attain a more thorough study of the critical heat flux and its validity with regards to the Shah "upstream conditions correlation" however, more mixed data points would need to be gathered since this is where z_{crit} was measured more accurately across a large range of mass flow rates and heat fluxes. Moreover, more testing is also required in order to determine if channel surface roughness has a measurable effect on the critical heat flux.

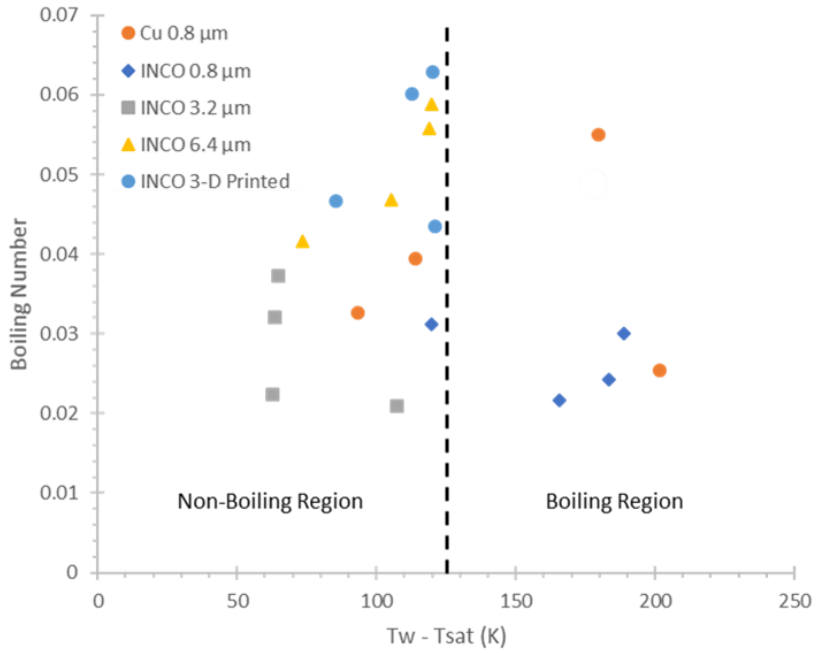

Figure 6.5: Boiling Number as a Function of Wall Temperature Minus Saturated Temperature

As a last part of this study, the plot found in Figure 6.6 was generated illustrating the measured Nusselt number versus the predicted Nusselt number based on Cook's correlation [18]. This correlation is based on an experimental investigation conducted by Cook in 1984. In this investigation, a Nusselt number correlation for supercritical CH_4 flowing through smooth channels was generated. Cook's correlation is unique because it includes a correction factor based on a T_b

to T_w ratio [19]. Furthermore, Huzel and Huang also presented a temperature correction factor based on a T_b to T_w ratio, described for "heat transferred through a vapor film boundary layer" for supercritical propellants [20]. Combining the knowledge from these two investigations, a temperature correction factor was utilized for this study's LN_2 tests, since it is assumed that heat is being transferred through a vapor film boundary layer in the subcooled film-boiling regime. Note that the measured Nusselt number only includes the convective heat transfer. As evident through Figure 11, the film-boiling data points lined up well with the non-boiling regime when the T_b/T_w correction factor was used. Moreover, the film-boiling data also lined up well with the rest of the points because the temperature correction factor accounts for the heat transferred through a vapor film boundary layer [18].

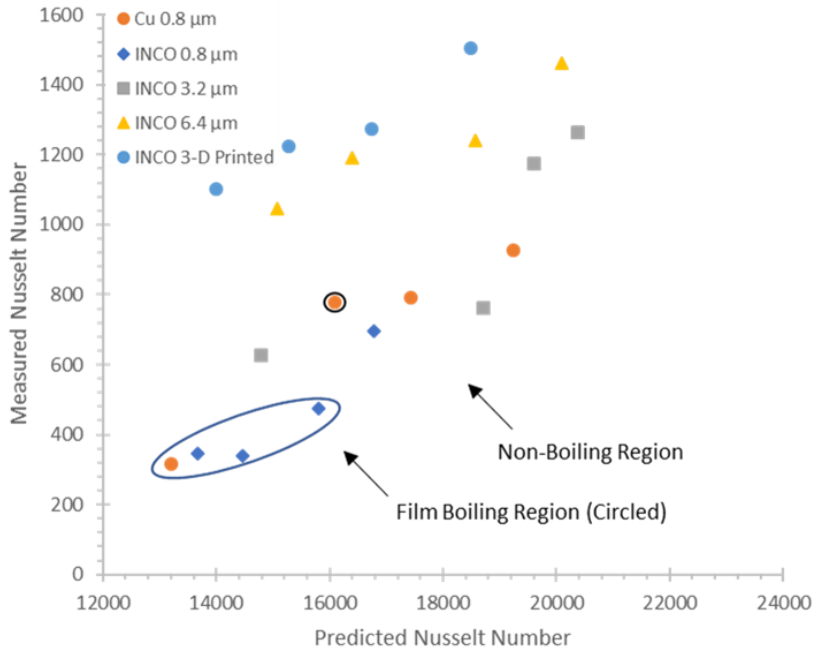

Figure 6.6: Measured Nusselt Number as a Function of Predicted Nusselt Number as per Cook's Correlation [19]

Chapter 7: Conclusions

7.1. Conclusion

An upgraded experimental setup of the High Heat Flux Test Facility was validated and the steady-state heat transfer characteristic of subcritical LN_2 were studied for Inconel 625 square channels with a cross-section of 3.2 x 3.2 mm and varying surface roughness. Additionally, an additively manufactured Inconel 625 channel was also tested in order to further expand on the effects of surface roughness on cooling effectiveness.

The data showed that subcooled film-boiling phenomena was present in all of the channels tested in this study and the critical heat flux is shown to occur at a boiling number of approximately $Bo \sim 0.06$. Furthermore, through the use of two different Nusselt number correlations, is was evident that channel cooling effectiveness increases as surface roughness increases in the non-boiling region; that is cooling effectiveness increases at the expense of increased pressure drops caused by larger channel roughness finishes. Since the additively manufactured channel possessed the largest surface roughness, it is concluded that it was the channel with the highest cooling effectiveness. Note that the measured Nusselt number took into account the convective heat transfer, while the predicted Nusselt number as per Cook's correlation took into account the heat transferred to a vapor film boundary layer by using the correction factor based on a T_b to T_w ratio.

7.2. Future Work

Although the data trends generated in this study agree with the original hypothesis that heat transfer increases with increasing surface roughness, more testing is recommended using more additively manufactured channels. The reason for this is because additive manufacturing methods incorporate different processes such as heat treating, that may very potentially affect the material's mechanical properties. Hence, by conducting more studies on different additively manufactured

test specimens, an assessment may be made on the effects that the additive manufacturing process has on the material's mechanical properties, more specifically thermal conductivity.

References

[1] Neill, T. Judd, D. Veith, E. and Rousar, D. 2009. Practical Uses of Liquid Methane in Rocket Engine Applications. Acta Astronautica, Vol. 65, pp. 696-705.

[2] Morehead, R.L. 2011. Project Morpheus Main Engine Development and Preliminary Flight Testing.Rocket Engine Applications. Acta Astronautica, Vol. 65, pp. 696-705.

[3] Barry, Patrick. "Methane Blast." NASA Science News. http://science.nasa.gov/sciencenews/Science-at-nasa/2007/04may_methaneblast/

[4] Oberg, E., et al. 2012. Machinery's Handbook. 29th ed. Industrial Press, New York, 2012, p. 739.

[5] Duesberg, J. 2012. Rocket TechnologyL: Thrust Chamber. http://www.kmaekris.gr/Rocket Technology/ThrustChamber. Boeing Engineering.

[6] Van Noord, J. 2010. A Heat Transfer Investigation of Liquid and Two-Phase Methane. NASA Glenn Research Center, NASA/TM-2010-216918, Cleveland, OH.

[7] Cook, R.T. 1984. Methane Heat Transfer Investigation. NASA Marshall Space Flight Center, NASA-CR-171199, Huntsville, AL.

[8] Gage, M. L. and Rosenberg, S. D. 1990. Hydrocarbon Fuel/Combustion-Chamber-Liner Materials Compatibility. NASA Lewis Research Center. NASA CR-185203, Cleveland, OH.

[9] Mass, E. Irvine S. A. Bates, R. and Auyeung T. 2004. A High Heat Flux Facility Design for Testing of Advanced Hydrocarbon Fuel Thermal Stability. Air Force Research Laboratory, 4847, Edwards AFB, CA.

[10] Trejo, A., Trujillo, A., Galvan, M., and Choudhuri, A., "Experimental Investigation of Methane Convection and Boiling in Rocket Engine Cooling Channels," *50th AIAA/ASME/SAE/ASEE Joint Propulsion Conference and Exhibit,* AIAA Paper 2014-8722, 2014.

[11] Trujillo, A. 2014. An Experimental Investigation of Liquid Methane Convection and Boiling In Rocket Engine Cooling Channels. UTEP Center for Space Exploration Technology Research, El Paso, TX.

[12] Bates, R. W. Mass, E. D. Irvine, S. A. and Auyeung, T. P. 2004. Design of a High Heat Flux Facility for Thermal Stability Testing of Advanced Hydrocarbon Fuels. Air Force Research Laboratory, F04611-99-C-0025, Edwards AFB, CA.

[13] Irvine S.A., and Burns R.M. 2005. Preliminary Heat Transfer Characteristics of RP-2 Fuel As Tested in the High Heat Flux Facility. Air Force Research Laboratory, AFRL-PR-ED-TP-2005-545, Edwards AFB, CA.

[14] Bates, R.W., Billingsley, M.C., and Lyu, H.Y. 2007. Experimental and Numerical Investigation of RP-2 Under High heat Fluxes. Air Force Research Laboratory, AFRL-PR-ED-TP-2007-150, AFB, CA.

[15] Trejo, A., Garcia, C., and Choudhuri, A., "Experimental Investigation of Transient Forced Convection of Liquid Methane in a Channel at High Heat Flux Conditions," Experimental Heat Transfer, Vol. 29, No. 1, 2016, pp. 97-112.

[16] Becker, M., *Heat Transfer: A Modern Approach,* 1st ed., Plenum, New York, 1986, p. 174.

[17] Fast, R.W., *Advances in Cryogenic Engineering: Part A and B,* Cryogenic Engineering Conference, 1st ed., Plenum, New York, 1960, p. 885.

[18] Cook, R.T. 1984. Methane Heat Transfer Investigation. NASA Marshall Space Flight Center, NASA-CR-171199, Huntsville, AL.

[19] Collier, J.G., and Thome, J.R., *Convective Boiling and Condensation,* 3rd ed., Oxford Science Publ., Oxford, England, U.K., 1996, p. 359.

[20] Huzel, D. and Huang, D. 1992. Modern Engineering for Design of Liquid-propellant Rocket Engines, Volume 147, American Institute of Aeronautics and Astronautics, Washington, D.C.

Appendix

List of Instrumentation

Item	Make	Model	Range	Accuracy	Use	Quantity
0.125" OD exposed tip type E thermocouple	Omega Engineering	EMQSS-125E-6	-200 to 900ºC (-328 to 1652ºF)	1.7ºC or 0.5% above 0ºC 1.7ºC or 1.0% below 0ºC	Test section wall temperature measurement	6
0.040" OD exposed tip type E thermocouple	Omega Engineering	EMQSS-040E-6	-200 to 900ºC (-328 to 1652ºF)	1.7ºC or 0.5% above 0ºC 1.7ºC or 1.0% below 0ºC	Heated wafer temperature measurement	6
0.125" OD ungrounded type E thermocouple	Omega Engineering	EMQSS-125U-6	-200 to 900ºC (-328 to 1652ºF)	1.7ºC or 0.5% above 0ºC 1.7ºC or 1.0% below 0ºC	Fluid inlet/outlet and line temperature measurement	3
0.040" OD sheathed type K thermocouple	Dalton Electric	TC-KG40D080L012	-200 to 900ºC (-328 to 1652ºF)	1.7ºC or 0.5% above 0ºC 1.7ºC or 1.0% below 0ºC	Cartridge heater surface temperature measurement	17
Thin Film Cryogenic Pressure Transducer	Omega Engineering	PX1005L-500AV	0 to 3.45 MPa (0 to 500 psia)	±0.25%	Fluid inlet/outlet and line pressure measurements	4
Thermocouple Input Module DAQ Device	National Instruments	NI 9213	Refer to Manual	Refer to Manual	Thermocouple data acquisition	2
Terminal Block with SCC Expansion Slots DAQ Device	National Instruments	NI SCC-68	Refer to Manual	Refer to Manual	Pressure transducer and flow meter data acquisition	1
Pressure Transducer Process Meter and Controller	Omega Engineering	DP25B-E-A	0 to 100 mV	±0.02% of reading	Pressure transducer signal conditioning	4
Convection-Enhanced Pirani Sensor	Kurt J. Lesker	K31714S	1.0×10^{-3} to 1.0×10^{3} Torr (1.9×10^{-5} to 19 psi)	±<1%	Vacuum chamber pressure measurement	1
Digital Convection Pirani Vacuum Gauge Controller	MKS	HPS 947	1×10^{-3} to 1×10^{3} Torr (1.9×10^{-5} to 19 psi)	±<1%	Vacuum chamber digital reading	1

Technical Drawing for New Heating Block Design

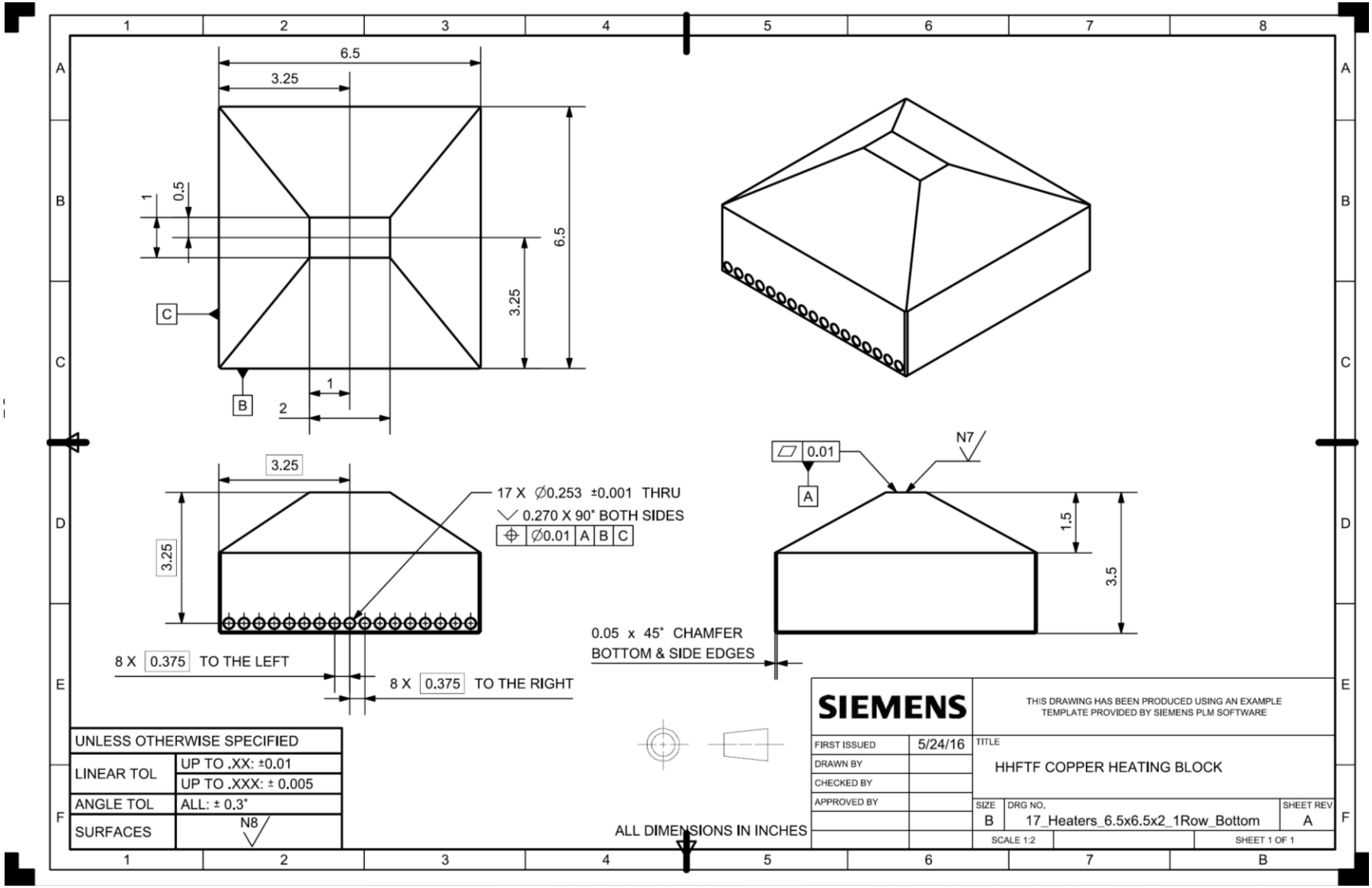

Detailed Experimental Procedure

** The following experimental procedure follows the instrumentation definition (names/numbers) as illustrated by Figure 3.2 and Figure 4.6 of this work. **

Pre-Experimental Procedure

1. Safety Protocol
    a. Put on appropriate personal protective equipment (PPE).
        i. Lab Coat
        ii. Steel Toe Boots
        iii. Goggles
    b. Take other safety precautions as needed.
        i. Tie long hair
        ii. Hold back loose clothing
        iii. Remove any articles of loose jewelry
2. Preparation of High Heat Flux Test Facility (HHFTF)
    a. Mount HHFTF on Test Stand
        i. Place Unifrax 1600 High Temperature Paper Insulation (thickness 0.0394") on the test stand's four small plates supporting and making contact with the bottom four corners of the copper block.
        ii. Carefully place the copper block on top of the four insulated supporting plates.
        iii. Place the aluminum wafer on top of the copper block.
        iv. Place the test sample on top of the aluminum wafer.
        v. Place Unifrax 1600 High Temperature Paper Insulation (thickness 0.0394") on cradle's section that will make contact with the test sample.
        vi. Place the cradle on top of the test sample.
        vii. Ensure that the cradle, test sample, and wafer are well aligned with the top area of the copper block.
    b. Engage Downward Pressure Mechanism on HHFTF
        i. Tighten bolts to apply pressure between the test sample, wafer, and copper block.
            1. Torque required per bolt: 36 ± 2 lbf-in
            2. This torque is the calculated result when using the pressure required for good conduction for an aluminum-copper interface. (i.e. 725 ± 5 psi applied pressure is needed to provide a good conduction interface and hence minimize conduction losses.)
    c. Instrumentation Placement
        i. Place one 0.040" OD sheathed type K thermocouple inside of the groove of each cartridge heater.
        ii. Insert one cartridge heater with its respective thermocouple inside each of the slots on the copper block.

iii. Place one 0.040” OD exposed tip type E thermocouple on each groove on both the block and test sample. There are a total of six grooves (3 on top of the copper block and 3 at the bottom of each test sample). Refer to the section entitled “High Heat Flux Test Facility”.
iv. Place one 0.125” OD exposed tip type E thermocouple on each of the six slots found on top of the test sample.

d. Interface Lines
   i. Place the test stand and HHFTF assembly inside of the vacuum chamber.
   ii. Connect the inlet and outlet lines of the test sample using the already available Swagelok connections.

3. Inspection/Preparation of Instrumentation and Equipment
   a. Electrical Instrumentation
      i. Turn on power supplies and adjust to required voltages.
         1. Solid State Relays: 5 VDC
         2. Solenoid Valves: 12 VDC
         3. Flow Meter Transmitter: 12 VDC
      ii. Connect solid state relays to 120 VAC extension cords.
      iii. Use a multi-meter to check for the proper functionality of all cartridge heaters by measuring the resistance across each solid state relay.
         1. Resistance across each solid state relay per group of 3 cartridge heaters is 12 ± 1 ohm.
      iv. Use the continuity option on the multi-meter to ensure that all thermocouples are making contact with their respective surface.
      v. Ensure that all pressure transducers and thermocouples are reading ambient conditions.
         1. Thermocouples: 77 ± 3ºF
         2. Pressure Transducers: 13 ± 1 psi
   b. System Leak Check
      i. Low-End Pressure Leak Check (50 psi)
         1. Connect facility air compressor to MV1 inlet.
         2. Fully open MV1 and SV2 valves.
         3. Turn on the facility air compressor to pressurize the lines.
            a. PT1 through PT4 should read 55 ± 5 psi.
         4. Apply Snoop Leak Detector fluid at all line joints.
         5. Tighten appropriate fittings in the case of any fluid bubbles forming.
         6. Disconnect the facility air compressor at the end of the leak check.
         7. Open NV1 valve to vent system.
         8. Fully close MV2, SV2, and NV1 valves.
      ii. High-End Pressure Leak Check (300 psi)
         1. Connect GN2 k-bottle to the inlet of MV1.
         2. Fully open MV1 and SV2 valves.
         3. Open the GN2 k-bottle tank valve.
            a. Regulate pressure to 300 psi.

4. PT1 through PT4 should read 300 ± 5 psi.
5. Monitor pressures closely to ensure that there are no significant pressure drops over time.
    a. Run leak check for at least 5 minutes.
6. Close the GN2 tank valve.
7. Open NV1 valve to vent system.
8. Fully close MV2, SV2, and NV1 valves.

c. System GN2 Purge
    i. Fully open MV1, SV2, and NV1 valves.
    ii. Open the GN2 k-bottle tank valve.
        1. Regulate pressure to 50 psi.
    iii. Ensure that all air is expelled from the system.
        1. Minimum Purge Run Time: 30 seconds.
    iv. Close the GN2 k-bottle tank valve.
    v. Fully close MV2, SV2, and NV1 valves.

Experimental Procedure

1. Prepare File Directory for Data Acquisition
    a. Run the LabVIEW program entitled "High Heat Flux Test Facility" located in the "LabVIEW programs" folder found on the computer's desktop.
    b. Ensure that LabVIEW program outputs the data file into the folder entitled "Liquid Nitrogen Test Data" also found on the computer's desktop.
2. Prepare for Data Collection
    a. Create a folder in the "Liquid Nitrogen Test Data" folder that specifies the conditions to be tested.
3. Pull Vacuum to HHFTF
    a. Close the vacuum chamber and secure it with its door latch to ensure a proper seal.
    b. Connect the vacuum pump to the vacuum chamber using the available O-Ring connection.
    c. Turn on the vacuum pump.
    d. Activate the Pirani vacuum gauge controller and monitor the vacuum chamber pressure until it reaches the desired levels.
        i. Min. Allowable Chamber Vacuum Level: 0.05 Torr
4. Begin Data Recording Process
    a. Change "Record On" switch to "ON" position on the GUI.
5. Heat up Copper Based Thermal Concentrator (Block)
    a. Turn on cartridge heaters.
    b. Heat up the block until desired temperature is reached.
        i. Refer to test matrix and monitor T24, T25, and T26.
            1. Accepted tolerances for these readings: ± 5 ^{o}F
            2. Estimated time to reach desired temperatures is 40 minutes.

ii. Temperature may be controlled by turning off heaters from the system as required, using their respective manual electrical switch.

6. Pre-Chill System
    a. Put on cryogenic personal protective equipment.
        i. Apron
        ii. Gloves
        iii. Face Mask
    b. Allow Liquid Nitrogen Flow into the System
        i. Open SV2 solenoid valve.
        ii. Open the LN2 dewar tank valve and regulate dewar pressure to the desired conditions.
            1. PT1 should read 100 ± 2 psi.
            2. System will be chilled at a lower pressure than operating pressures in order to acquire a lower (colder) temperature prior to regulating the dewar to operating pressures.
        iii. Open NV1 needle valve.
        iv. Allow LN2 to flow through the test sample and into the dewar exhaust collector.
            1. Monitor T2 until it reaches -275 ± 2ºF.
        v. Open SV1 solenoid valve.
        vi. Gradually open MV2 manual valve.
7. Throttle System to Desired Mass Flow Rate
    a. Regulate dewar pressure to the desired conditions using the LN2 dewar valve.
        i. Refer to test matrix and monitor PT1.
    b. Adjust NV1 needle valve to the desire mass flow rate.
        i. Refer to test matrix for desired flow rate and monitor the flow meter reading.
        ii. Readings from PT2, PT3, T1, and T2 will serve as a backup mass flow rate reading (check) in the case that the flow meter over spins.
    c. Monitor the test sample's skin temperatures until the readings reach steady state conditions.
        i. Steady State conditions are acceptable when sample readings are within 1 ºF from each other for **each** thermocouple (T27, T28, T29, T30, T31, and T32).
8. Ensure data contains at least 20 seconds of steady state data.
9. Close Off Liquid Nitrogen Flow
    a. Close the LN2 dewar valve.
10. End Data Recording Process
    a. Change "Record On' switch to "OFF" position on the GUI.
11. Turn off vacuum.
12. Open vacuum chamber by opening its door latch.
    a. Wait a minimum of 40 minutes to ensure that HHFTF is cooled down to ambient conditions (i.e. T4-T32 should all read ambient conditions: 77 ± 3ºF.)

b. If necessary, take out the test stand and HHFTF assembly from the vacuum chamber and replace the test sample following the assembly instructions found in Step 2 under the section entitled “Pre-Experimental Procedure”.

13. Repeat steps 1 – 12 from this section “Testing Procedure” for each test sample and each data point on the test matrix.

Post-Experimental Procedure

1. Monitor System Pressures and Temperatures
    a. Thermocouples: 77 ± 3ºF
    b. Pressure Transducers: 13 ± 1 psi
2. Deactivate All Electronic Devices
    a. Disconnect vacuum pump from vacuum chamber.
    b. Test the functionality of the cartridge heaters by checking their resistance.
    c. Disconnect SSR (relays) from 120 VAC extension cords.
    d. Turn off power supplies.

Emergency Procedure

All safety considerations were taken and an emergency procedure was developed in case of an unwanted occurrence. Red lines are shown to avoid a catastrophic failure of the hardware or facilities.

Red Lines

- Line pressures must remain less than 350 psia.
    - PT1, PT2, PT3, and PT4 should read less than 350 psia.
    - If any pressure exceed the red lines, close the main dewar/tank valve source.
- Block temperatures must remain less than 930ºF.
    - T21-T26 should read less than 930ºF.
    - If any temperatures exceed the red lines, turn off all cartridge heaters.
- Cartridge heater temperatures must remain less than 900ºF.
    - T4-T20 should read less than 650ºF.
    - If any temperatures exceed the red lines, turn off all cartridge heaters.

Risks and Hazards

Hazard	Risk	Mitigation
Cryogenics	Cold contact burns, explosion due to pressure build-up, asphyxiation.	Cryogenic PPE, pressure relief valves, oxygen monitor device.

In the event of an emergency:

- Close LN2 source.
- Relieve residual system pressure: “Post-Test Procedure”.
- Deactivate all electronic devices: “Post-Test Procedure”.
- Inform other teams of the situation.
- Evacuate the lab if necessary.
- Contact Luz Bugarin at (915) 747-7398.
- If life/facility in danger, call UTEP police (915) 747-5611.

Vita

Armando Sandoval Jr was born and raised in El Paso, Texas. He attended the University of Texas at El Paso beginning in Fall of 2011, and worked as an undergraduate research assistant studying multifunctional materials during the last two years of his undergraduate studies. In 2015, he earned a Bachelor of Science Degree in Mechanical Engineering and immediately after began pursuing a Master of Science Degree in Mechanical Engineering. As a graduate student, Armando worked as a research assistant at the Center for Space Exploration Technology Research, and interned at NASA Johnson Space Center in the summer of 2016 working towards the development of LOX-Methane Propulsion Systems. In the Fall of 2017, he accepted an offer from White Sands Missile Range to begin his career as an engineer. Armando has since been working full-time, while completing his Master of Science Degree in Mechanical Engineering. In the future, he plans on enrolling in a doctoral program to pursue a degree in Mechanical Engineering with a focus in deep space propulsion systems.

Permanent Address: 11728 Snow Hawk Dr.

El Paso, TX 79936

This thesis was typed by Armando Sandoval Jr